Palaeontologia Electronica
palaeo-electronica.org

An analysis of the first fossil remains of styracosternan ornithopod dinosaurs from the Early Cretaceous of La Rioja (Spain) and its paleobiogeographical implications

Juan García-Palou, Erik Isasmendi, and Angélica Torices

ABSTRACT

La Rioja, located in the eastern sector of the Cameros Basin, has one of the highest concentrations of Lower Cretaceous dinosaur ichnites in the Iberian Peninsula. However, the skeletal remains of these animals are scarce and only the presence of carcharodontosaurid and spinosaurid theropods in the Enciso Group and hypsilophodontid ornithopods in the Oliván Group are known. This paper describes and analyses fossil remains found at the El Horcajo site from the Oncala or Enciso Group and attributes them to styracosternan ornithopod dinosaurs. If confirmed, these results suggest that these are the earliest styracosternan remains from the Cameros Basin and from other Lower Cretaceous deposits from the Iberian Peninsula, indicating this group inhabited the Iberian Peninsula 7.2 million years before previously acknowledged.

Juan García-Palou. MUCBO | Museu Balear de Ciències Naturals, FJBS-MBCN, ctra. Palma-Port de Sóller km 30,5, 07100 Sóller, Islas Baleares, España. (corresponding author) jgarcia@mucbo.org
Erik Isasmendi. Departamento de Geología/Geología Saila, Facultad de Ciencia y Tecnología/Zientzia et Teknologia Facultatea, Universidad del País Vasco/ Euskal Unibertsitatea (UPV/EHU). Barrio Sarriena, s/n, 48940 Leioa, Bizkaia 48940, España. erik.isasmendi@ehu.eus
Angélica Torices. Departamento de Geodinámica, Estratigrafía y Paleontología, Universidad Complutense de Madrid. Planta 2ª, C. de José Antonio Novais, 12. 28040 Madrid, España. atorices@geo.ucm.es

Keywords: Early Cretaceous; Cameros Basin; Paleobiogeography; Dinosauria; Ornithopoda; Styracosterna

Submission: 16 December 2023. Acceptance: 22 July 2025.

Final citation: García-Palou, Juan, Isasmendi, Erik, and Torices, Angélica. 2025. An analysis of the first fossil remains of styracosternan ornithopod dinosaurs from the Early Cretaceous of La Rioja (Spain) and its paleobiogeographical implications. Palaeontologia Electronica, 28(2):a34.
https://doi.org/10.26879/1364
palaeo-electronica.org/content/2025/5599-styracosternan-of-la-rioja

INTRODUCTION

The Lower Cretaceous deposits of the Cameros Basin in La Rioja area of Spain are widely known for the richness of their dinosaur ichnites (Díaz-Martínez, 2013; Pérez-Lorente, 2015; García-Ortiz de Landaluce, 2016). On the other hand, dinosaur skeletal remains from the Early Cretaceous are rare and have only been found in two lithostratigraphic units in the Riojan sector of the Cameros Basin. The first is the Enciso Group, where the fossil remains of *Riojavenatrix lacustris* have been described (Isasmendi et al., 2024), as well as other fossil remains referable to Spinosauridae (Navarro-Lorbés and Torices, 2018; Isasmendi et al., 2020; 2023) and Carcharodontosauridae (Navarro-Lorbés and Torices, 2018). The second is the Oliván Group, where remains of cf. *Hypsilophodon* sp. have been found (Torres and Viera, 1994; Ruiz-Omeñaca, 2001). Dinosaur eggshells have also been reported in the Lower Cretaceous deposits of the Cameros Basin and have been referred to the ornithopod oogenus *Guegoolithus turolensis* (Moreno-Azanza et al., 2016). However, in the Riojan sector of the Cameros Basin, skeletal remains of large ornithopods have not yet been described in detail.

This paper describes new ornithopod dinosaur remains found in the El Horcajo site (Oncala or Enciso Gr), in La Rioja. These fossil remains have also been systematically analyzed and compared with other known ornithopod taxa. In addition, morphometric analyses have been performed to quantitatively compare them with other Iberian and European members of Ornithopoda. Finally, the paleobiogeographical implications of these results are considered within the current knowledge of styracosternan ornithopods of Europe (Appendix 1) and the Iberian Peninsula (Appendix 2).

GEOGRAPHICAL AND GEOLOGICAL SETTING

The dinosaur skeletal remains presented here were found in the locality of Trevijano (central La Rioja), in northern Spain (Figure 1A). The El Horcajo site is situated 1 km west of the village of Trevijano.

Geologically, this site is in the northeastern part of the Cameros Basin (Figure 1B). This basin mainly developed in the second rifting stage that

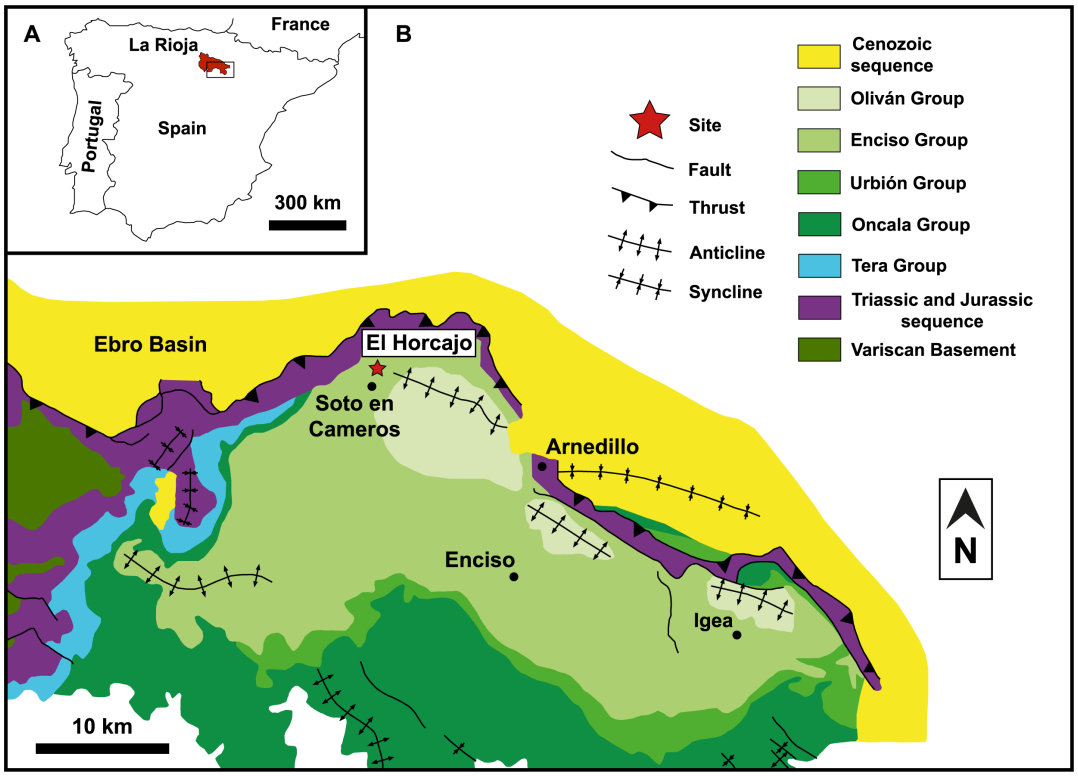

FIGURE 1. Location of La Rioja and the sites; A, geographical map of the Iberian Peninsula; B, geological map of the northeastern Cameros Basin and location of the El Horcajo site (modified from Suárez-Gonzalez et al., 2013 and Isasmendi et al., 2021).

occurred during the Late Jurassic and Early Cretaceous in the Iberian Mesozoic Rift (Mas et al., 2002). The Cameros Basin can be divided into two smaller sub-basins, the Eastern Cameros sub-basin and the Western Cameros sub-basin (Mas et al., 1993; 2003). The deposits of the Cameros Basin are mainly continental or coastal in origin, reaching up to 6,500 m in thickness in the depocenter of the basin (Martin-Chivelet et al., 2019 and references therein). These deposits are Tithonian–early Aptian in age (Martin-Chivelet et al., 2019 and references therein) and have been traditionally divided into Tera, Oncala, Urbión, Enciso, and Oliván groups (Figure 1B) by Tischer (1966). Nevertheless, Mas et al. (2002) proposed eight sedimentary sequences (DS 1-8), where the fluvial deposits evolve laterally and upwards to more lacustrine environments (Hernán, 2018).

The El Horcajo area (Figure 1B) has been proposed as being part of either the Oncala (DS 3 of Mas et al., 2002) or Enciso groups with no currently agreed consensus (e.g., Doublet, 2004; Schudack and Schudack, 2009; Suárez-Gonzalez et al., 2013). In any case, the El Horcajo stratigraphic levels consist of grey marls within a red clay-grey marl interval interpreted as being formed in a lacustrine-palustrine system, with coastal influence (Moreno-Azanza et al., 2016). In the El Horcajo site, the fossils were found in situ in a siltstone bed (Figure 2).

Regarding the age of the Enciso Gr, different ranges have been proposed based on different studies. However, the lack of high resolution biostratigraphic data hinders the absolute dating of the unit. The most recent studies date the Enciso Gr as latest Barremian-early Aptian (Suárez-González et al., 2013). The chronostratigraphy carried out in the El Horcajo fossil site dates it to the Valanginian–Hauterivian (Moreno-Azanza et al., 2016), regardless of the lithostratigraphic unit it belongs to.

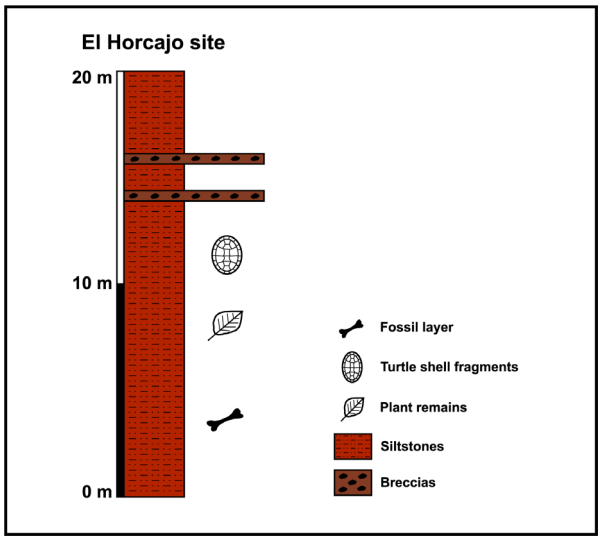

FIGURE 2. The El Horcajo site stratigraphic column (modified from Moreno-Azanza et al., 2016).

MATERIAL AND METHODS

Material

The fossil remains studied in this work were found at the El Horcajo site. These remains were recovered during a survey carried out in 2008 by the research teams of the University of La Rioja and Aragosaurus. These fossils were accumulated in an area of about 20 square meters, near each other, and were extracted by digging shallowly into the sediment (Moreno-Azanza, pers. comm.). Fossils from this site comprise an anterior caudal vertebra (CP 411), mentioned in Moreno-Azanza et al. (2016), a proximal fragment of a humerus (CP 412), a proximal carpal fragment (radiale) (CP 414), a mid-distal portion of the shaft of a left tibia (CP 415), and a proximal fragment of a fibula (CP 413). All these fossils are housed at the Centro Paleontológico de Enciso in Enciso (La Rioja, Spain).

Comments on the state of preservation of the material. At the site of the El Horcajo, dinosaur eggshells, an ornithopod vertebra, the teeth of theropod dinosaurs and crocodylomorphs, and fish scales have been recovered (Moreno-Azanza et al., 2016; Navarro-Lorbés and Torices, 2018). In this site, bone remains such as the vertebra and others, which make up the set studied in this work, are presented as fragmentary, abraded, and incomplete bones. Due to the relative size ratio of the five fossils studied from this site, it is proposed that four of them could be associated with a single individual, while another one would belong to a different individual (See Taxonomic assignment and number of individuals). Despite the unfavorable state of preservation, all the skeletal remains present limited but sufficient characters to be identified and compared taxonomically.

Methods

These fossil remains were systematically studied and compared with other ornithopod taxa. This task has been carried out through the first-hand study of the fossil remains deposited in different institutions in Spain (see Appendix 3), and the

review of the available literature data of the fossils deposited in the institutions of other countries.

The variables measured for the anterior caudal vertebra CP 411 were: vertebral centrum length (L); height of the anterior articular facet of the centrum (Ha); height of the posterior articular facet of the centrum (Hp); width of the anterior articular facet of the centrum (Wa); width of the posterior articular facet of the centrum (Wp). The variables measured for the appendicular elements CP 412, CP 413, CP 414, and CP 415 were: length (L); width (Wa); height (H). The anatomical nomenclature of Ramírez-Velasco and Alvarado-Ortega (2022) has been used for describing part of the material, as well as for anatomical structures. A section with anatomical justifications for the anatomical assignments of the most fragmentary fossils is added.

For systematic comparisons, the phylogeny proposed by Poole (2022) for Ornithopoda has been adopted in this work. For the anatomical identification, location and orientation of the tibial fragment (CP 415), 3D models of appendicular elements of ornithopods were reviewed using MorphoSource software.

A multivariate analysis has also been performed, consisting of a Principal Component Analysis (PCA), comparing the anterior caudal vertebra (CP 411) with data obtained from measurements of the anterior caudal vertebrae of other ornithopod taxa (see Appendix 4), which have been normalized to base 10 logarithms. PAST v4.03 (Hammer et al., 2001) software was used to process the statistical data obtained from the measurements. CP 411 was the only specimen complete enough to allow sufficient variables to be compared with known taxa. Comparable measurements in these taxa were obtained by taking first-hand data in some specimens and consulting published supplementary material for other taxa. In cases where there is no supplementary material with fossil measurements of the specimens, measurements have been taken using ImageJ software (Rueden et al., 2017) using published figures.

Institutional Abbreviations

CP, Centro Paleontológico de Enciso, Enciso, Spain; **MAP**, Museo Aragonés de Paleontología, Teruel, Spain; **MNS**, Museo Numantino, Soria, Spain; **NHMUK**, Natural History Museum, London, United Kingdom; **MDS**, Museo de Dinosaurios de Salas de Los Infantes, Salas de Los Infantes, Spain).

SYSTEMATIC PALEONTOLOGY

DINOSAURIA Owen, 1842
(sensu Poole, 2022)
ORNITHISCHIA Seeley, 1887
(sensu Poole, 2022)
NEORNITHISCHIA Cooper, 1985
(sensu Poole, 2022)
ORNITHOPODA Marsh, 1881
(sensu Madzia et al., 2021)
IGUANODONTIA Dollo, 1888
DRYOMORPHA Sereno, 1986
(sensu Poole, 2022)
ANKYLOPOLLEXIA Sereno, 1986
(sensu Poole, 2022)
STYRACOSTERNA Sereno, 1986
(sensu Poole, 2022)
Styracosterna indet.

Axial Skeleton

Caudal vertebra. CP 411 belongs to an anterior caudal vertebra (Figure 3A-F). The caudal vertebra preserves its centrum, part of base of the neural spine, and the bases of the caudal ribs. The centrum is platycoelous, laterally compressed, and dorsoventrally elongated. The edges of the articular facets are damaged (Figure 3A, B).

The centrum is sub-rectangular in lateral view and dorsoventrally taller than anteroposteriorly wide (Figure 3C, D). The anterior haemal facet faces anteroventrally at an angle of 30º with respect to the anterior articular facet (Figure 3A, C), whereas the posterior articular haemal facet is posteroventrally oriented with an angle of approximately 50º with respect to the posterior articular facet (Figure 3B, D). Both haemal facets are lateromedially wider than anteroposteriorly long (Figure 3A, B). A nutritional foramen is present on both sides of the vertebral centrum (Figure 3C, D). Only on the left lateral surface (Figure 3C), fusion marks between the neural arch and the vertebral centrum are present (neurocentral synchondrosis). The neural canal is spindle shaped in the anteroposterior direction (Figure 3A, B). The caudal ribs are incomplete, but they seem to be dorsolaterally projected (Figure 3A, B). The bases of the caudal ribs are elliptical in outline with the anteroposterior axis being the longest. The CP 411 vertebra is identified as an anterior caudal (Figure 3G) due to the dorsoventrally higher than anteroposteriorly long centrum, presence of caudal ribs, and well-developed facets for the haemal arches. The measurements of CP 411 can be seen in Table 1.

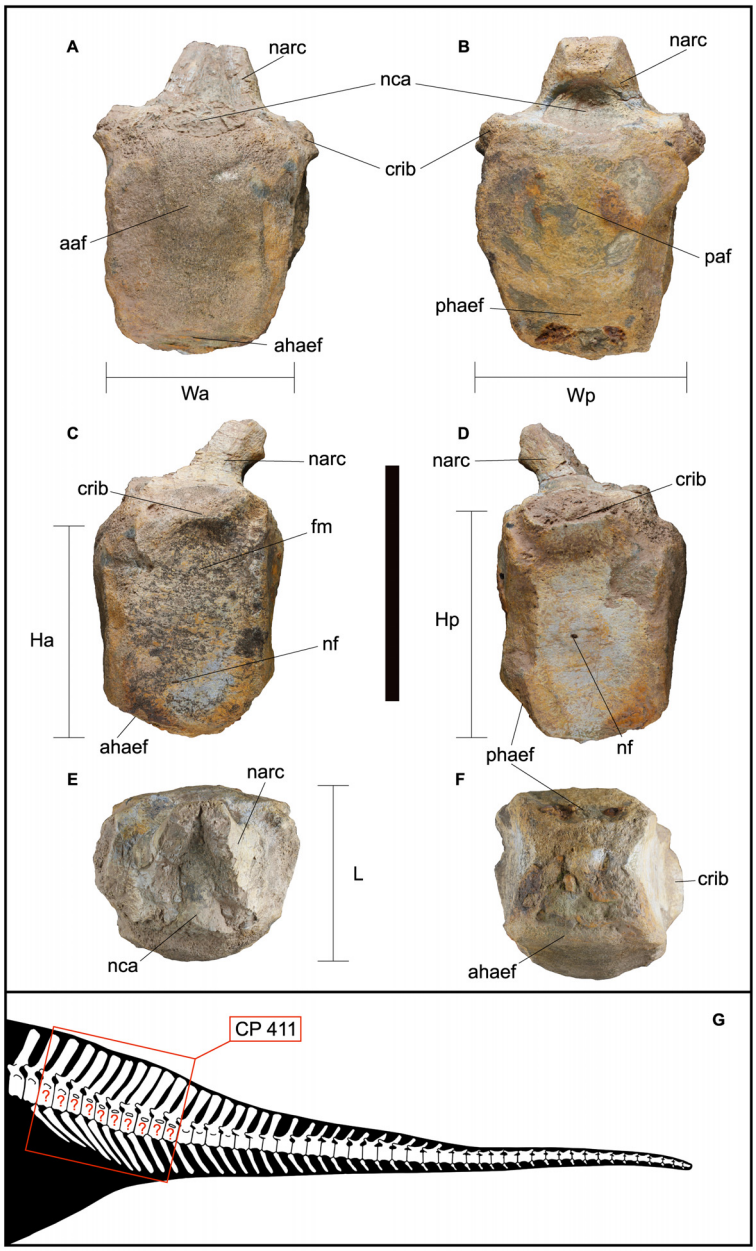

FIGURE 3. Anterior caudal vertebra CP 411: A, anterior view; B, posterior view; C, left lateral view; D, right lateral view; E, dorsal view; F, ventral view; G, position of CP 411 between the anterior caudal vertebrae showing transverse processes of the caudal series (modified from Scott Hartman, 2016). The question symbol (?) indicates the plausible precise location. Abbreviations: *aaf*, anterior articular facet; *ahaef*, anterior articular haemal facet; *crib*, caudal rib; *fm*, fusion marks; *Ha*, height of the anterior articular facet of the centrum; *Hp*, height of the posterior articular facet of the centrum; *L*, vertebral centrum length; *narc*, neural arch; *nca*, neural canal; *nf*, nutritional foramen; *paf*, posterior articular facet; *phaef*, posterior articular haemal facet; *Wa*, width of the anterior articular facet of the centrum; *Wp*, width of the posterior articular facet of the centrum. Scale bar equals 10 cm.

TABLE 1. Measurements (in mm) of CP 411. Abbreviations: *Ha*, height of the anterior articular facet of the centrum; *Hp*, height of the posterior articular facet of the centrum; *L,* vertebral centrum length; *Wa,* width of the anterior articular facet of the centrum; *Wp*, width of the posterior articular facet of the centrum.

Code	Element	L	Wa	Ha	Wp	Hp
CP 411	Anterior caudal vertebra	58.0	80.0	75.0	75.0	75.0

Appendicular Skeleton

Humerus. CP 412 is a fragment of the proximal end of a left humerus (Figure 4A-E). In anterior view, the anterior surface of the element is flat (Figure 4A). In posterior view, this bone preserves part of the humeral head, which is bulging and rounded, and part of the medial tuberosity, which is flat, but the lateral tuberosity is absent (Figure 4B). From the base of the humeral head, following a straight line to the medial edge of the bone, the surface is raised, possibly due to bone regrowth (Figure 4B). In proximal view, CP 412 presents a slightly curved profile mediolaterally, as well as part of the regrowth, which protrudes slightly from the dorsal face, and part of the humeral head which is also abraded (Figure 4C). The distal view exhibits the fracture surface between CP 412 and the rest of the humerus, which is also abraded, and the bone tissue is rough (Figure 4D). The measurements of CP 412 can be seen in Table 2.

The anatomical identification of CP 412 as a fragment of left proximal humerus (Figure 4E) is due to the general morphology of the fossil, as well as the identification of the condyle of the most proximal part of the fragment as the humeral head (Figure 4B-D). The hypothesis that CP 412 could belong to a fragment of another type of appendicular element of similar size such as a scapula, coracoid, ilium, or pubis has been excluded. CP 412 differs from the anterior end of a scapula or coracoid because it has a sub-rectangular and curved morphology in anterior and posterior view (Figure 4A, B), whereas in a coracoid the anterior end is broad and expanded in *Iguanodon bernissartensis* (Norman, 1980), roughly rectangular in *Mantellisaurus atherfieldensis* (Bonsor et al., 2023), or flat, broad, and very thick in *Magnamanus soriaensis* (Fuentes-Vidarte et al., 2016). In addition, the posteriorly protruding proximal end (humeral head) also does not morphologically resemble either a glenoid, ventral process, or acromion process. The glenoid forms a large crescent-shaped concave depression in *I. bernissartensis* (Norman, 1980) and is arc-shaped in *Mantellisaurus atherfieldensis* (Bonsor et al., 2023); the ventral process is a pronounced hook-shaped ridge, while the acromion process is also hook-shaped in *Mantellisaurus atherfieldensis* (Bonsor et al., 2023).

CP 412 also differs morphologically from an ilium or pubis, because of its protruding proximal end; in a pubis, the thickness decreases posteriorly until the prepubic process (e.g., *I. bernissartensis* [Norman, 1980], or *Mantellisaurus atherfieldensis* [Bonsor et al., 2023]), whereas in CP 412 the thickness remains homogeneous throughout the fragment. In the case of an ilium, the mediolateral thickness remains constant, but the shape of this bone, which is more elongated anteroposteriorly than higher proximodistally in ornithopods such as *I. bernissartensis* (Norman, 1980), *Mantellisaurus atherfieldensis* (Bonsor et al., 2023), *Ouranosaurus nigeriensis* (Bertozzo et al., 2017), or *Morelladon beltrani* (Gasulla et al., 2015), differs from CP 412, which is sub-rectangular and curved.

Carpal. CP 414 has been attributed to a left proximal fragment of a carpal bone, specifically a radiale, due to the morphology of the proximal concavity, corresponding to the radius facet, and the distal concavity, corresponding to the facet for metacarpal II (Figure 5A). The radiale is worn and incomplete, and only the proximal end is preserved. In anterior view (Figure 5A), the fragment presents a subrectangular morphology with concave proximal and distal facets due to the radius facet and the facet for metacarpal II. The radius facet is more concave compared to the metacarpal facet (Figure 5A). The facet for metacarpal II is also smooth. Both the dorsal and ventral faces are flat (Figure 5B, D). The radiale is thicker ventrally and dorsally and in posterior view (Figure 5C), the fracture surface is observed, as well as the cancellous bone tissue. The surface of the radial facet is smooth, and the edges have striations, which mark the morphologically anatomical dorsoventral limits of the radius facet (Figure 5E). In proximal and distal views, CP 414 presents a half-oval-shaped morphology due to the absence of the rest of the radiale (Figure 5E, F). The measurements of CP 414 can be seen in Table 3.

The anatomical assignment of CP 414 to a left proximal fragment of a carpal bone, specifically a radiale (Figure 5A-F), is due to the presence of two concaved facets, one on the proximal face and one on the distal face, which have been identified as the radius facet and the facet for metacarpal II. The hypothesis that CP 414 could belong to a manual or pedal phalanx has been discarded. It can be observed that manual phalanges in ornithopoda usually present flat (e.g., *Ouranosaurus nigeriensis*, Bertozzo et al., 2017) or concave (e.g., *Mantellisaurus atherfieldensis*, Bonsor et al., 2023) articular faces vary in proximodistal length, depending on whether there are proximal or distal phalanges, and present an hourglass-shaped morphology in anterior, posterior, and lateral and medial view. In the pedal phalanges of ornithopods, it is observed that the proximal articular faces are usually concave, and the distal ones con-

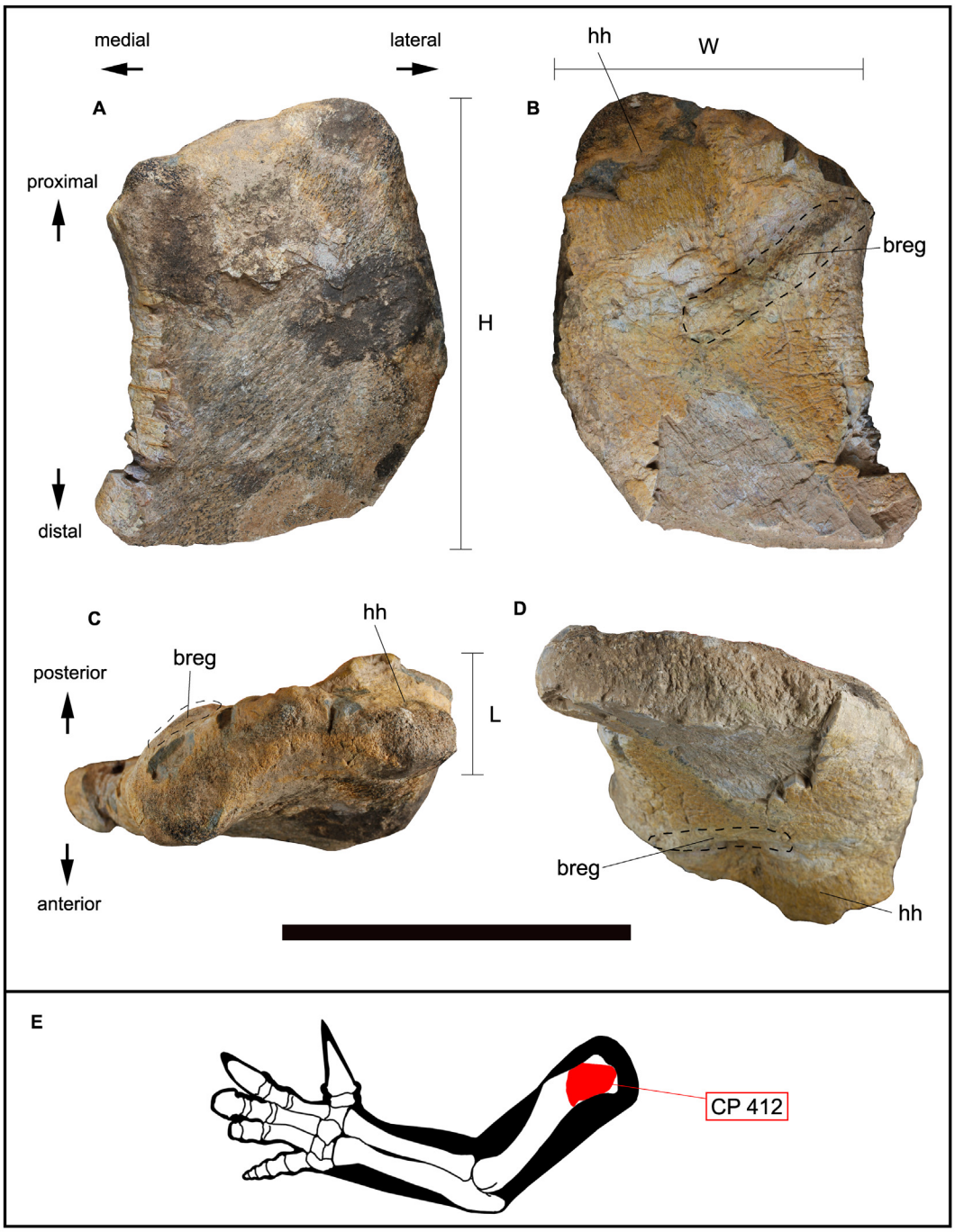

FIGURE 4. Fragment of proximal end of left humerus CP 412: A, anterior view; B, posterior view; C, proximal view; D, distal view; E, position of CP 412 on the left humerus (modified from Scott Hartman, 2016). Abbreviations: *breg*, bone regrowth; *H*, height; *hh*, humeral head; *L*, length; *W*, width. The morphology of the dashed lines is indicative; it does not indicate a precise morphology. Scale bar equals 10 cm.

TABLE 2. Measurements (in mm) of CP 412. Abbreviations: *H*, height; *L*, length; *W*, width.

Code	Element	W	H	L
CP 412	Left proximal humerus fragment	100.0	160.0	30.0

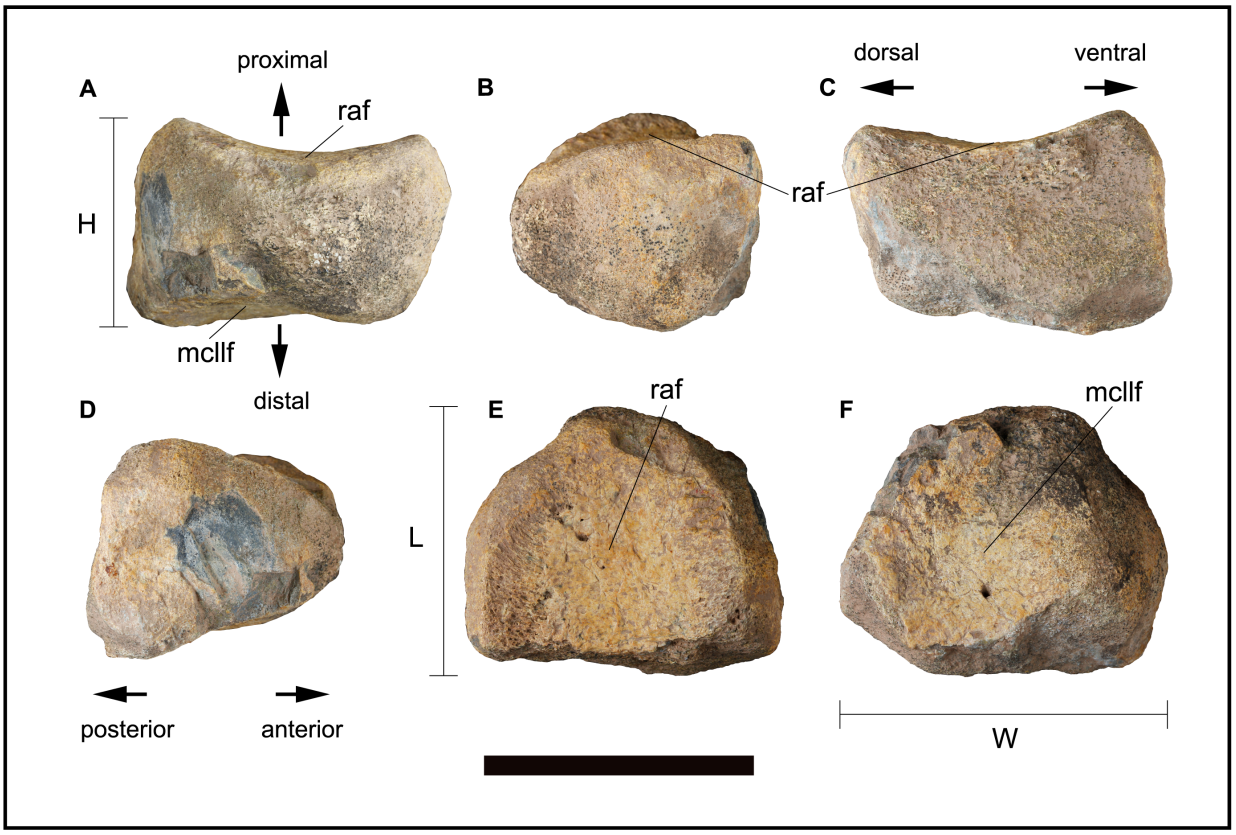

FIGURE 5. Left proximal carpal fragment (radiale) CP 414: A, anterior view; B, dorsal view; C, posterior view; D, ventral view; E, proximal view; F, distal view. Abbreviations: *H*, height; *L*, length; *mcI*, metacarpal I; *mcIIf*, metacarpal II facet; *raf*, radius facet; *W*, width. Scale bar equals 5 cm.

vex (e.g., *Ouranosaurus nigeriensis* [Bertozzo et al., 2017]; *Mantellisaurus atherfieldensis* Bonsor et al., 2023]), and as with the manual phalanges, the morphology in anterior, posterior, lateral and medial view is hourglass-shaped. In CP 414 both articular faces are concave, and although it is true that in anterior and posterior view the morphology may look like an hourglass, in lateral and medial view the morphology is subtriangular, so that morphologically it is not consistent with a manual or pedal phalanx.

Tibia. CP 415 corresponds to a mid-distal portion of the shaft of a left tibia (Figure 6A-G) and is slightly taller (Figure 6A-D) than wide (Figure 6E, F). The section perpendicular to the major axis cross-section of the shaft is teardrop-shaped, wider laterally, and narrowing medially until reaching the medial surface which is adjacent to the fibula (Figure 6E, F). The compact bone is maximum 1 cm in thickness, as well as the medullary cavity. The measurements of CP 415 can be seen in Table 4.

The assignment of CP 415 to a mid-distal tibial diaphysis (Figure 6G) has been made after comparing the general morphology of the bone, in different views, with digitized models of other appendicular bones of ornithopod dinosaurs (see Methods). The hypothesis that CP 415 could belong to a diaphysis or intermediate section of another type of appendicular long bone such as a femur, humerus, radius, ulna, or fibula has been ruled out. This is because examining the section morphology of 3D models of elongate appendicular bones of other ornithopods, such as those of the digitized specimen of *Mantellisaurus atherfielden-*

TABLE 3. Measurements (in mm) of CP 414. Abbreviations: *H*, height; *L*, length; *W*, width.

Code	Element	W	H	L
CP 414	Left proximal carpal fragment (radiale)	60.0	40.0	45.0

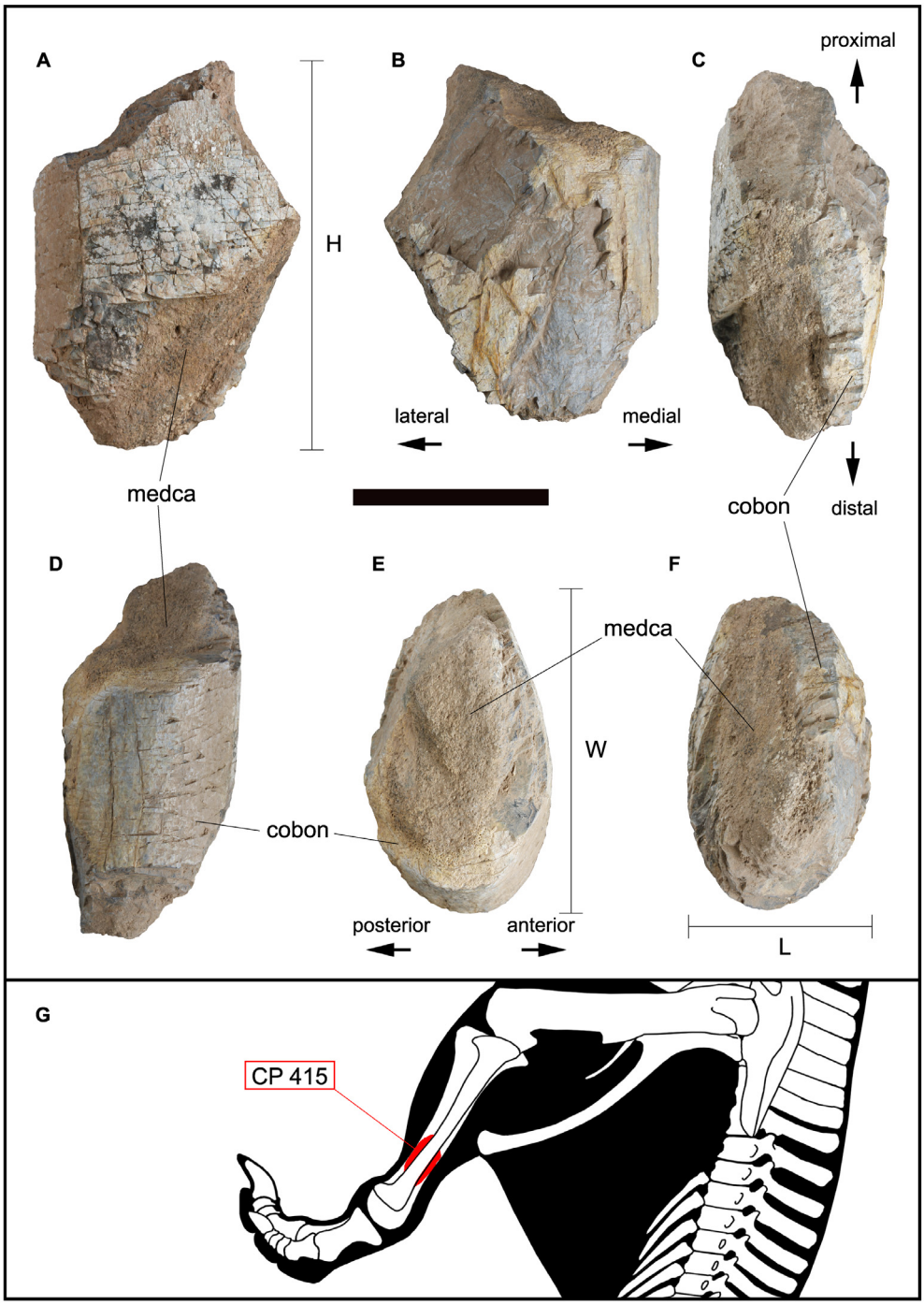

FIGURE 6. Left tibia CP 415: A, anterior view; B, posterior view; C, lateral view; D, medial view; E, proximal view; F, distal view; G, position of CP 415 on the left tibia (modified from Scott Hartman, 2016). Abbreviations: *cobon*, compact bone; *H*, height; *medca*, medullary cavity; *L*, length; *W*, width. Scale bar equals 5 cm.

TABLE 4. Measurements (in mm) of CP 415. Abbreviations: *H*, height; *L*, length; *W*, width.

Code	Element	W	H	L
CP 415	Mid-distal portion of shaft of a left tibia	80.0	85.0	45.0

sis NHMUK PV R5764 (Morphosource/ Mantellisaurus) shows that the drop-shaped morphology of CP 415, seen in proximal and distal view (Figure 6E, F), does not agree with any morphology that a femoral or humeral diaphysis section may have. The femur sections vary constantly in shape along the diaphysis, while in the humerus, the diaphysis of the distal part presents a subellipsoidal section morphology, also differing from CP 415. In the case of the section morphologies of the radius diaphysis, it does not agree with CP 415, mainly due to the size and thickness of CP 415. Furthermore, the radius diaphysis sections present a subrounded morphology, with the medial surface wedged, also differing from CP 415. The section perpendicular to the major axis of the diaphysis of the ulna of *Mantellisaurus atherfieldensis* (digitalized specimen NHMUK PV R5764) presents a subrounded morphology, which is consistent longitudinally throughout the bone. In the fibula, the diaphysis sections of the proximal part present a rounded morphology, while the distal diaphysis is subrounded. None of these morphologies in the diaphysis sections of these two bones coincide with the one presented by CP 415.

Fibula. CP 413 belongs to a proximal fragment of a left fibula (Figure 7A-E), specifically to the mid-posterior part of the *caput fibulae* (sensu Baumel and Witmer, 1993; Ramírez-Velasco and Alvarado-Ortega, 2022) (Figure 7A, C). The cranial process and the rest of the distal part of the fibula are absent, the posterior edge of the fibula is slightly curved in a proximodistal direction (Figure 7A, C). In posterior view, the fragment is elongated proximodistally and flattened lateromedially (Figure 7B). In proximal view the posterior border is rounded (Figure 7D), the *facies articularis tibialis* (sensu Baumel and Witmer, 1993; Ramírez-Velasco and Alvarado-Ortega, 2022) is almost flat, while the *facies articularis femoralis* (sensu Baumel and Witmer, 1993; Ramírez-Velasco and Alvarado-Ortega, 2022) forms a slight curve in the anteroposterior direction (Figure 7D). In lateral and medial views, the *facies articularis femoralis* and the *facies articularis tibialis* exhibit an inverted subtriangular morphology (Figure 7A, C). However, this is the result of the fractured margins of the bone and the missing cranial process. The measurements of CP 413 can be seen in Table 5.

The anatomical identification of CP 413 as a left proximal fragment of fibula (Figure 7E) is due to the general morphology of the fossil, where one of the longitudinal faces corresponds to the *facies articularis femoralis* and the one on the opposite side to the *facies articularis tibialis*. These features have allowed us to identify the fossil as the middle-posterior part of a *caput fibulae*. The morphology of CP 413 may partly resemble that of a medial process of an ulna, but this hypothesis has been discarded because in CP 413, the proximal surface and the posterior curvature are joined by a rounded corner (Figure 7A, C), whereas in the medial processes of the ulnae of ornithopods such as *Ouranosaurus nigeriensis* (Bertozzo et al., 2017) or *Mantellisaurus atherfieldensis* (Norman, 1986; Bonsor et al., 2023), these corners are angular. It should also be noted that in proximal view, the thickness of the medial processes of the ulnae increases mediolaterally, while in CP 413, despite the wear, the anatomical thickness of the bone is maximal in the anteroposterior medial axis of the fragment (Figure 7D). Furthermore, the thickness decreases progressively on both sides, which differs from that of a medial process of an ulna.

RESULTS

Morphometric Analysis (PCA)

In this PCA, the total variance is explained by five principal components (PCs) (see Appendix 4). PC1 describes 98.03% of the total variance, with the main variable being the Hp, followed by the Ha, Wp, Wa, and L. The second principal component with the most weight is PC2, which describes 0.88% of the total variance, the variable with the most weight being Hp, followed by Ha and L. The parameters Wa and Wp present the values closest to zero, being those that present proportionally less weight in PC2. The morphospace of Styracosterna indet. (Morphotype I) overlaps completely with that of *Magnamanus soriaensis*, and with part of that of the styracosternans *Brighstoneus simmondsi, Mantellisaurus atherfieldensis, Ouranosaurus nigeriensis,* and *Hypselospinus* cf. *fittoni* (Figure 8). It also overlaps with part of the morphospecies of the dryosaurid *Valdosaurus canaliculatus* and CP 411 (Figure 8). The morphospace of the hadrosauriform *Comptonatus chasei* only partially overlaps with that of *Brighstoneus simmondsi* (Figure 8). The morphospaces of cf. *Hypsilophodon* sp. and Rhabdodontomorpha are far from the rest of the ornithopods without any overlap (Figure 8). In general, this diagram shows that styracosternans and hadrosauriformes are mostly located, and quite overlapping each other, in the second and fourth quadrants, while dryosaurids, hypsilophodontids, and rhabdodontomorphs are mostly scattered in the third quadrant (Figure 8). This diagram shows a

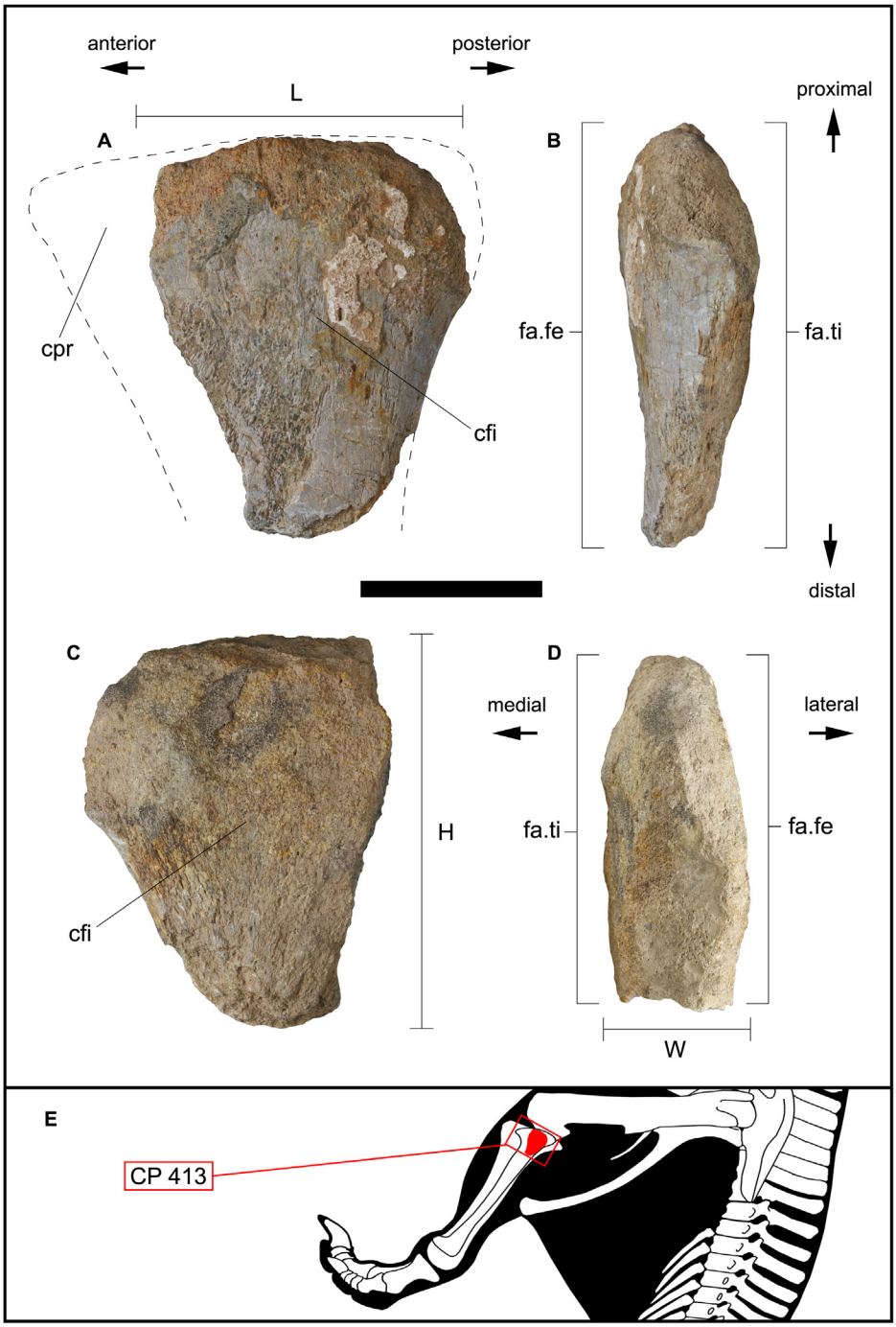

FIGURE 7. Left proximal fibula fragment CP 413: A, lateral view; B, posterior view; C, medial view; D, proximal view; E, position of CP 413 on the left fibula (modified from Scott Hartman, 2016). Abbreviations: *cfi*, caput fibulae*; cpr*, cranial process; *fa.fe*, facies articularis femoralis; *fa.ti,* facies articularis tibialis; *H*, height; *L*, length; *W*, width. Scale bar equals 5 cm.

TABLE 5. Measurements (in mm) of CP 413. Abbreviations: *H*, height; *L*, length; *W*, width.

Code	Element	W	H	L
CP 413	Left proximal fibula fragment	28.0	85.0	70.0

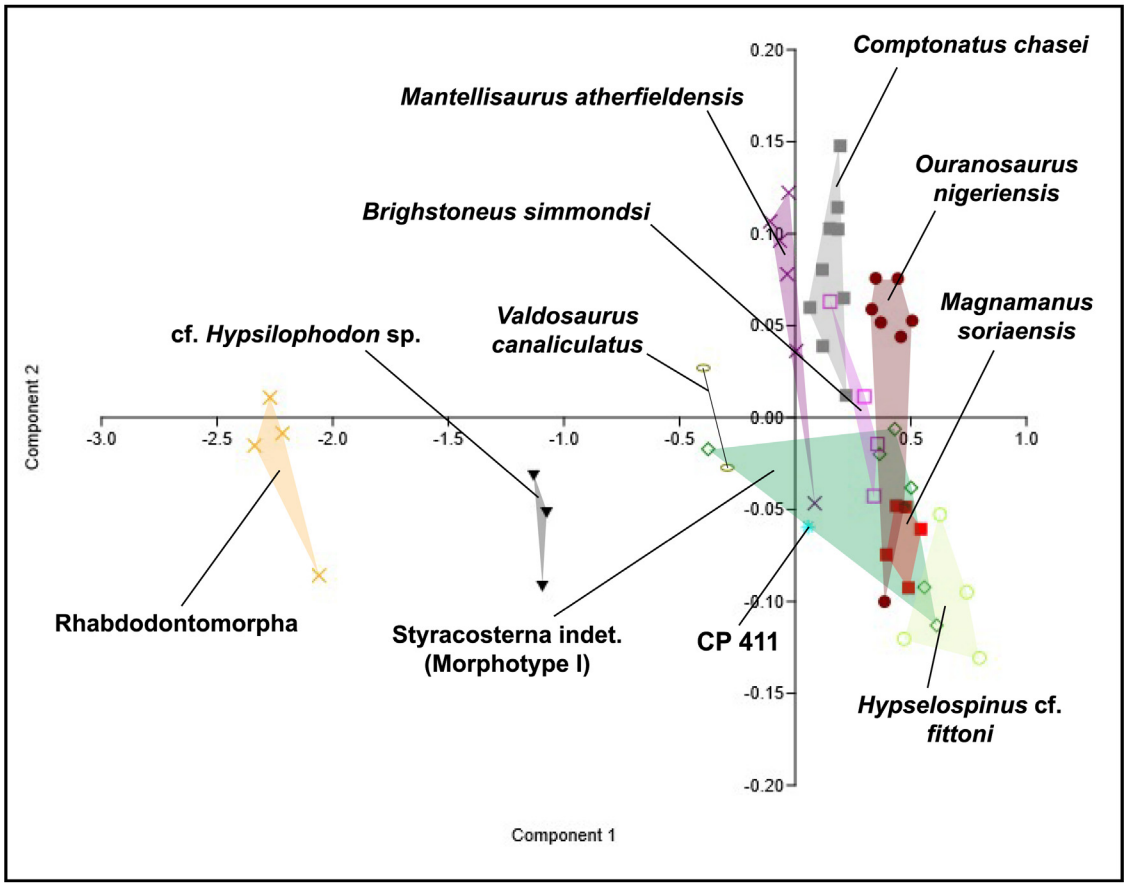

FIGURE 8. PCA diagram (PC1 Vs. PC2) of normalized linear measurements of caudal vertebral centra of CP 411, dryosauridae, hypsilophodontidae, rhabdodontomorpha, hadrosauriformes and styracosternan ornithopods.

first approximation of the variability of the anterior caudal vertebrae of the different types of Lower Cretaceous ornithopods. It shows that the anterior caudal vertebrae of the rhabdodontomorphs, hypsilophodontids and dryosaurids exhibit a more marked variability among them and with respect to the styracosternans and hadrosauriformes ornithopods, which show more homogeneous values among them. The values of the anterior caudal vertebra CP 411 are similar to those of the styracosternans analyzed, indicating a greater affinity with this type of ornithopod dinosaurs.

Taxonomic Assignment, Number of Individuals

Considering the current evidence and the similarities between the fossils examined and the ornithopod dinosaur taxa mentioned above, as well as considering the results of the PCA, the most likely interpretation is that the fossil remains from the El Horcajo site belong to styracosternan ornithopods. Thus, the fossils from this site have been assigned as belonging to indeterminate styracosternan ornithopods (Styracosterna indet.) (Figure 9).

If the remains from the El Horcajo site are compared with those of other more complete styracosternans, such as *I. bernissartensis* (Norman, 1980) and *Mantellisaurus atherfieldensis* (Bonsor et al., 2023), it is observed that the caudal vertebra (CP 411), the humerus (CP 412), the fibula (CP 413), and the distal middle portion of the shaft of a tibia (CP 415), present a similar size relationship, suggesting that they probably belonged to the same individual. Examining the size relationship between the radialia and the anterior caudal vertebrae and long bones from other more complete styracosternans such as *I. bernissartensis* (Norman, 1980), *Magnamanus soriaensis* (Fuentes-Vidarte et al., 2016), and *Mantellisaurus atherfieldensis* (Bonsor et al., 2023), it is observed that in these taxa the radialia are smaller than the caudal vertebrae and long bones (humerus, tibia, and fibula), being half or less than that of axial and appendicular elements. The size relationship between

FIGURE 9. Approximate reconstruction of the indeterminate styracosternan ornithopods found in the Early Cretaceous of the eastern Cameros Basin. Illustration by Adrián Blázquez Riola.

CP 414 with the rest of the material from El Horcajo is inverse to that observed for the previous cases, being proportionally equal or greater. Therefore, it is more likely that CP 414 belongs to a larger individual than the other elements.

Comparisons with Other Ornithopods

Caudal vertebra. The platycoelous centrum exhibited by CP 411 (Figure 10A-C) is also present in Iguanodontidae indet. (Torcida Fernández-Baldor et al., 2006) (Figure 10D, E), *I.* cf. *galvensis* (García-Cobeña et al., 2022) (Figure 10F, G), *Magnamanus soriaensis* (Fuentes-Vidarte et al., 2016) (Figure 10H, I), *Barilium* cf. *dawsoni* (Norman, 2011), in the Bernissart and Morella *I. bernissartensis* specimens (Norman, 1980; Gasulla et al., 2022) (Figure 10J, K), Styracosterna indet. (Morphotype I) (Verdú et al., 2019) (Figure 10L, M), *Cumnoria prestwichii* (Maidment et al., 2023), in *Hypselospinus* cf. *fittoni* (Norman, 2015), *Tenontosaurus tilletti* (Forster, 1990), *Zalmoxes robustus* (Weishampel et al., 2003), *Comptonatus chasei* (Lockwood et al., 2024), and *Eolambia caroljonesa* (McDonald et al., 2012a). However, the slightly concave articular facets of CP 411 centrum differ from *Rhabdodon priscus* (Chanthasit, 2010) and *Cumnoria prestwichii* (Maidment et al., 2023), whose anterior caudal vertebrae are amphicoelous. CP 411 also differs from *Iguanodon* cf. *galvensis* (García-Cobeña et al., 2022) (Figure 10F, G), *Ouranosaurus nigeriensis* (Bertozzo et al., 2017), *Mantellisaurus atherfieldensis* (Norman, 1986; Bonsor et al., 2023), and *Brighstoneus simmondsi* (Lockwood et al., 2021) because the latter exhibit amphiplatian anterior caudal vertebrae. CP 411 also differs from the shallowly convex morphology of the anterior caudal vertebrae of *Valdosaurus canaliculatus* (Barret, 2016) and slightly opisthocoelous centra found in rhabdodontomorphs (Dieudonné et al., 2016).

The anterior and posterior sub-rectangular articular facets of the centrum of CP 411 is shared with *I.* cf. *galvensis* (García-Cobeña et al., 2024), and it is comparable with those of the Bernissart specimens of *I. bernissartensis* (Norman, 1980) and *Mantellisaurus atherfieldensis* (Norman, 1986;

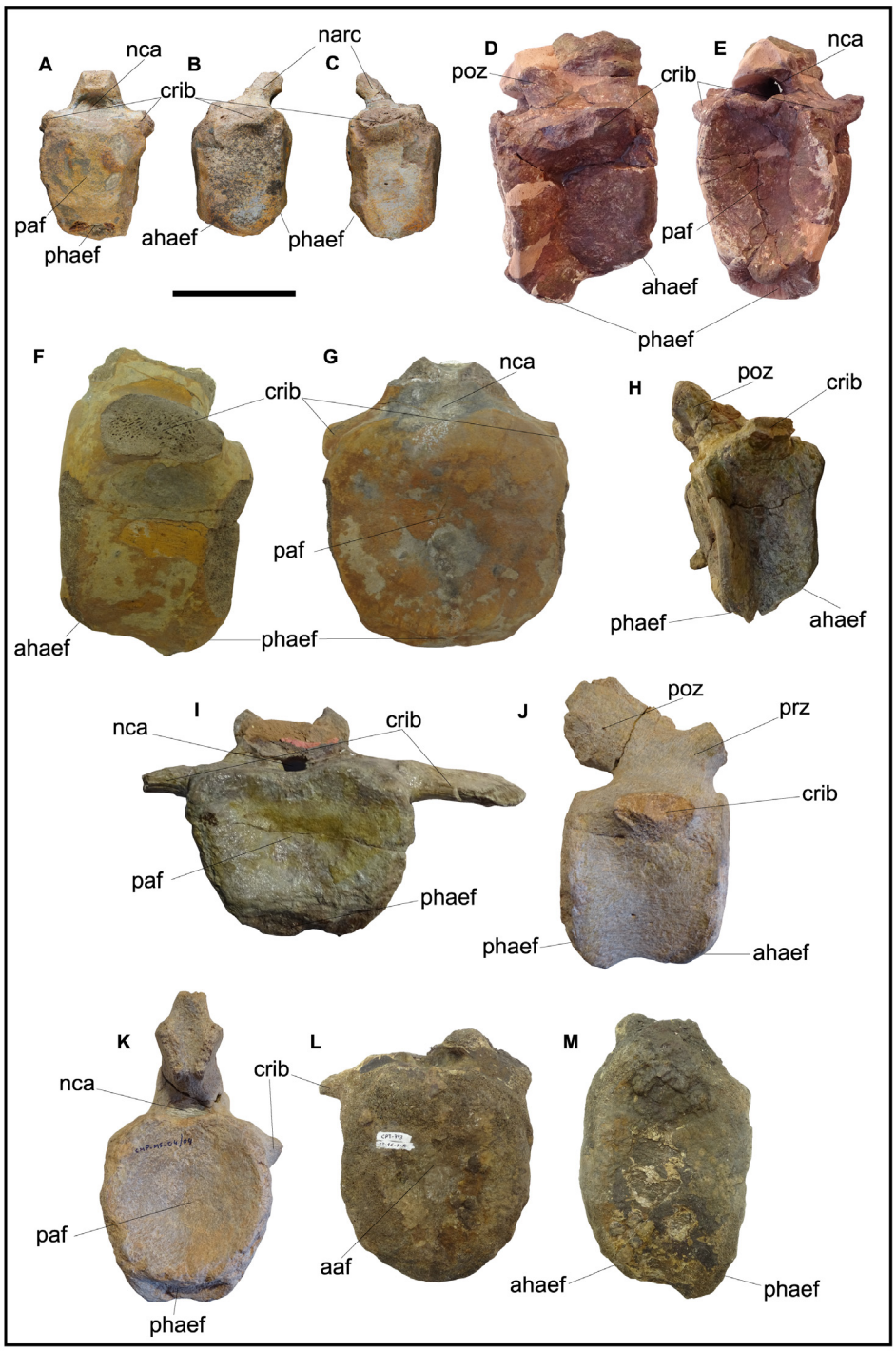

FIGURE 10. CP 411 compared to selected anterior caudal vertebrae of styracosternan ornithopods. CP 411: A, in posterior view; B, in left lateral view; C, in right lateral view. This work. Iguanodontidae indet. (MDS-TBMV, 7): D, in right lateral view; E, in posterior view. Photos taken from MDS-TBMV, 7 (Torcida Fernández-Baldor et al., 2006). *Iguanodon* cf. *galvensis* (MAP-8043): F, in left lateral view; G, in posterior view. Photos taken from MAP-8043 (García-Cobeña et al., 2022). *Magnamanus soriaensis* (MNS 2000/122.2): H, in right lateral view; I, in posterior view. Photos taken from MNS 2000/122.2 (Fuentes-Vidarte et al., 2016). *Iguanodon bernissartensis* (CMP-MS-04/04): J, in right lateral view; K, in posterior view. Photos taken from CMP-MS-04/04 (Gasulla et al., 2022). Styracosterna indet. (Morphotype I) (MAP-793): L, in anterior view; M, in left lateral view. Photos taken from MAP-793 (Verdú et al., 2019). Abbreviations: *ahaef*, anterior articular haemal facet; *crib*, caudal rib; *narc*, neural arch; *nca*, neural canal; *paf*, posterior articular facet; *poz*, postzygapophysis; *phaef*, posterior articular haemal facet; *prz*, prezygapophysis. Scale bar equals 10 cm.

Bonsor et al., 2023), where the anterior caudal vertebrae in both taxa are roughly rectangular. The shape of the articular surfaces of CP 411 differs from *Magnamanus soriaensis* (Fuentes-Vidarte et al., 2016) (Figure 10I), *Uteodon aphanoecetes* (Carpenter and Wilson, 2008), *Rhabdodon priscus* (Chanthasit, 2010), *Z. robustus* (Weishampel et al., 2003), and *Brighstoneus simmondsi* (Lockwood et al., 2021) because in the latter taxa the anterior caudal vertebrae are heart-shaped in anterior and posterior views.

The shape of the articular facets of CP 411 also differs from the Morella specimen of *I. bernissartensis* (Gasulla et al., 2022) (Figure 10K), *Barilium* cf. *dawsoni* (Norman, 2011), and *Hypselospinus* cf. *fittoni* (Norman, 2015) due to the sub-rounded shape of the anterior caudal vertebrae of the aforementioned taxa. The CP 411 articular facets shape also differs from *I.* cf. *galvensis* (García-Cobeña et al., 2022) (Figure 10G) and Rhabdodontomorpha (Dieudonné et al., 2016) due to its rounded morphology. The articular facets shape of CP 411 also differs from *Tenontosaurus tilletti* (Forster, 1990), *Eolambia caroljonesa* (McDonald et al., 2012a) and *Cumnoria prestwichii* (Maidment et al., 2023), which exhibit subcircular facets in anterior and posterior views. In the case of the Iguanodontidae indet. (Torcida Fernández-Baldor et al., 2006) (Figure 10E), the morphology of its caudal vertebrae is sub-ellipsoidal, that of *Comptonatus chasei* (Lockwood et al., 2024) is oval-shaped, that of *Ouranosaurus nigeriensis* (Bertozzo et al., 2017) is square-shaped, and that of Styracosterna indet. (Morphotype I) (Verdú et al., 2019) (Figure 10L) is sub-quadrangular, differing from CP 411.

Specimen CP 411 exhibits well-developed haemal facets (Figure 10B, C), with the posterior facet being more pronounced than the anterior one. This character is also found in the Bernissart and Morella *I. bernissartensis* specimens (Norman, 1980; Gasulla et al., 2022) (Figure 10J), *I.* cf. *galvensis* (García-Cobeña et al., 2024), *Ouranosaurus nigeriensis* (Bertozzo et al., 2017), Iguanodontidae indet. (Torcida Fernández-Baldor et al., 2006) (Figure 10D), *I.* cf. *galvensis* (García-Cobeña et al., 2022) (Figure 10F), *Mantellisaurus atherfieldensis* (Norman, 1986; Bonsor et al., 2023), Styracosterna indet. (Morphotype I) (Verdú et al., 2019) (Figure 10M), *Barilium* cf. *dawsoni* (Norman, 2011), *Hypselospinus* cf. *fittoni* (Norman, 2015), *Brighstoneus simmondsi* (Lockwood et al., 2021), *Comptonatus chasei* (Lockwood et al., 2024), *Tenontosaurus tilletti* (Forster, 1990), *Rhabdodon priscus* (Chanthasit, 2010), *Cumnoria prestwichii* (Maidment et al., 2023), *Uteodon aphanoecetes* (Carpenter and Wilson, 2008), *Valdosaurus canaliculatus* (Barret, 2016), and in the middle caudal vertebrae of *Zalmoxes robustus* (Weishampel et al., 2003). In the anterior caudal vertebrae of *Magnamanus soriaensis* (Fuentes-Vidarte et al., 2016) (Figure 10H) the anterior haemal facet is more developed than the posterior one, differing from CP 411.

Humerus. In posterior view, the morphology of CP 412 is similar to that present in the humeri of *Ouranosaurus nigeriensis* (Bertozzo et al., 2017), *Mantellisaurus atherfieldensis* (Bonsor et al., 2023), *I.* cf. *galvensis* (Verdú, 2017), in the hadrosauriform *Comptonatus chasei* (Lockwood et al., 2024), and in the hadrosauroid *Eolambia* (McDonald et al., 2012a). On the other hand, the degree of curvature of CP 412 differs from the Bernissart specimen of *I. bernissartensis* (Norman, 1980), *Uteodon aphanoecetes* (Carpenter and Wislon), and *Cumnoria prestwichii* (Maidment et al., 2023) because the medial profile that goes from the lateral tuberosity to the middle part of the humerus is rectilinear, differing morphologically with CP 412.

Carpal. The half-oval-shaped morphology in proximal and distal views of CP 414 resembles the morphology of the anterior end of the radiale of *Magnamanus soriaensis* (Fuentes-Vidarte et al., 2016) and *I. bernissartensis* (Norman, 1980). This crescent-shaped morphology of CP 414 differs from that of *Barilium* cf. *dawsoni* (Norman, 2011), which is square-shaped. In *Ouranosaurus nigeriensis* (Rasmussen, 1998), the facet for the radius is similar to that of CP 414, but the facet for metacarpal II is squarer in *Ouranosaurus*, differing from CP 414.

This morphology of CP 414 also differs from *Mantellisaurus atherfieldensis* (Bonsor et al., 2023), where the anterior end of the radiale presents a sub-ellipsoidal shape, from the radiale of the rhabdodontoid *T. tilletti* (Rasmussen, 1998), which presents a ‘’D-shape’’ and differs from *U. aphanoecetes* (Carpenter and Wilson, 2008), which presents a quadrangular shape.

The sub-triangular morphology of CP 414, in lateral and medial views, with a rounded anterior end, differs from all ornithopod radialia mentioned above, which present almost rectangular shapes, such as *Mantellisaurus atherfieldensis* (Bonsor et al., 2023), and *U. aphanoecetes* (Carpenter and Wilson, 2008), or almost square, such as in *Ouranosaurus nigeriensis* (Rasmussen, 1998), *Magnamanus soriaensis* (Fuentes-Vidarte et al.,

2016), and *I. bernissartensis* (Norman, 1980). In the case of *T. tilletti* (Rasmussen, 1998), in lateral view it is observed that the proximal facet is convex, and the distal facet is concave, differing greatly from CP 414.

Determining whether the posterior part of the radial is fused to other carpal bones forming one of the anatomical structures mentioned above, which cannot be answered with certainty given the present evidence.

Fibula. The sub-triangular morphology, as the slightly proximodistal curve of the *caput fibulae* CP 413 resembles those of *I. bernissartensis* (Norman, 1980), *Ouranosaurus nigeriensis* (Bertozzo et al., 2017) and *Mantellisaurus atherfieldensis* (Bonsor et al., 2023), while it differs from cf. *Hipsilophodon* sp. (Torres and Viera, 1994), whose posterior surface in the proximo-distal direction is straight. In Rhabdodontomorpha (Dieudonné et al., 2016) morphology is more subrectangular and the proximodistal curve is sigmoidal, while in *Z. robustus* (Weishampel et al., 2003) the morphology is almost rectangular and no curve is observed in the proximodistal direction at the posterior end, so both taxa also differ from CP 413.

DISCUSSION

Paleobiogeographical Implications

In Central, Northern, and Eastern Europe, several styracosternan ornithopods have been described in different lithostratigraphic formations and units (Appendix 1).

The oldest styracosternan ornithopod remains of this region come from the Valanginian deposits of the Vectian Basin in England (Hopson et al., 2008) (Appendix 1). The Vectian Basin is subdivided into the Weald and Wessex sub-basins. In the Weald sub-basin are the Wadhurst Clay, Tunbridge Wells Sand formations, and Weald Clay Formation, the first two dated as Valanginian, and the third one dated as Barremian (Batten, 2011; Austen and Batten, 2018). The Wadhurst Clay, Tunbridge Wells Sand and Weald Clay formations have yielded remains assigned to *Barilium* cf. *dawsoni* (Norman and Barret 2002; Norman, 2011, 2013), *Hypselospinus* cf. *fittoni* (Norman and Barret, 2002; Norman, 2013, 2015) and *Hypselospinus* cf. *fittoni* (Norman, 2015) (Appendix 1). In the Wessex sub-basin, the Barremian Wessex Formation (only the outcrops of the upper part in the Isle of Wight) and the Barremian-Aptian Vectis Formation (Batten, 2011; Austen and Batten, 2018) remains of *Brighstoneus simmondsi* (Lockwood et al., 2021), *I. bernissartensis* (Norman, 2011, 2015) and *Mantellisaurus atherfieldensis* (Norman, 1986; Bonsor et al., 2023) have been found (Appendix 1).

Remains attributed to *Iguanodon* sp. have been discovered in the eastern Paris Basin (France), specifically in the Hauterivian Calcaire à Spatangues and the Barremian Argiles Ostreénes formations (Buffetaut, 2004 and references therein) (Appendix 1). In the Mons Basin (Belgium), specifically in the Barremian Sainte-Barbe Clays Formation, remains of *I. bernissartensis* have been reported (Norman, 1980; Yans et al., 2006; Baele et al., 2012 and references therein) (Appendix 1).

In the Rhenish Massif (Germany), in the ‘’Nehden Clays’’, remains of *I. bernissartensis* and *Mantellisaurus atherfieldensis* (Norman, 1987) have been described (Appendix 1). The clays in which the fossils were buried, which had subsided into a karstic fissure system that involved Devonian limestones (Norman, 1987) have been comparatively dated as Aptian and are roughly penecontemporaneous with the Weald Clay Unit of the Wealden Formation of southeastern England and Bernissart (Norman, 1987).

In the Iberian Peninsula, many styracosternan ornithopods have been found in the different formations and lithostratigraphic units that make up the sedimentary basins and sub-basins of this southwestern European region (Appendix 2). In the western sub-basin of the Cameros Basin, in the Golmayo Formation, dated as late Hauterivian-early Barremian (Mas et al., 1993), remains attributed to *Magnamanus soriaensis* have been described (Fuentes-Vidarte et al., 2016) (Appendix 2). In the early Barremian Pinilla de los Moros Formation (Martín-Closas and Alonso-Millán, 1998), and the late Barremian-Aptian Castrillo de la Reina Formation (Martín-Closas and Alonso-Millán, 1998) of the same sub-basin, remains of indeterminate iguanodontids (Torcida Fernández-Baldor et al., 1996, 1999, 2006) have been discovered (Appendix 2). This work now adds styracosternan records for the Eastern sub-basin in the El Horcajo site, from the Oncala? or Enciso? group, which is dated as Valanginian-Hauterivian in age (Moreno-Azanza et al., 2016) (Appendix 2).

In the Maestrazgo Basin, numerous remains of styracosternan ornithopods also have been reported (Appendix 2). In the Peñagolosa subbasin, in the El Castellar Formation, dated as early Hauterivian-Barremian in age (Martín-Closas, 1989), remains attributed to Styracosterna indet. (Verdú et al., 2019; García-Cobeña et al., 2022, 2023) and *Iguanodon* cf. *galvensis* (García-

Cobeña et al., 2022) have been studied (Appendix 2). In the Galve sub-basin, in the early Barremian Camarillas Formation (Martín-Closas, 1989; Villanueva-Amadoz et al., 2015), remains of *I.* cf. *galvensis* (Verdú et al., 2015, 2019; García-Cobeña et al., 2024) and *Delapparentia turolensis* (Ruiz-Omeñaca, 2011; Gasca et al., 2015) have been discovered (Appendix 2). In the Oliete sub-basin, specifically in the Escucha Formation, dated as late Aptian-early Albian (Rodríguez-López et al., 2009), remains of *Proa valdearinoensis* (McDonald et al., 2012b) and Styracosterna indet. (Rey et al., 2018) have been described (Appendix 2). In the same sub-basin, but in the Barremian Blesa Formation (Riveline et al., 1996; Aurell et al., 2018), remains of Styracosterna indet. have also been reported (Medrano-Aguado et al., 2022) (Appendix 2). In the Morella sub-basin, specifically in the Arcillas de Morella Formation, belonging to the early Aptian (Santafé et al., 1982; Salas et al., 2001), ornithopod remains attributed to *I. bernissartensis* (Gasulla et al., 2010, 2014, 2022; Gasulla, 2015), *Mantellisaurus atherfieldensis* (Gasulla et al., 2012; Gasulla, 2015), *Morelladon* (Gasulla et al., 2015) and Styracosterna indet. (Gasulla, 2015) have been found (Appendix 2).

In the South Iberian Basin, specifically in the Cuenca sub-basin, remains of styracosternan ornithopods have also been reported (Appendix 2). In the Barremian-early Aptian La Huérguina Formation from the Southiberian Basin (Martín-Chivelet et al., 2002; Poyato-Ariza et al., 2016), remains attributed to *Mantellisaurus atherfieldensis* (Llandres-Serrano et al., 2013) have been studied (Appendix 2). In the same sub-basin, but in the late Barremian of the Tragacete Formation (Buscalioni et al., 2008; Fregenal-Martínez et al., 2017), remains attributed to I. *bernissartensis* (Sanguino and Buscalioni, 2018) and I. cf. *bernissartensis* (Berrocal-Casero et al., 2025) have been found (Appendix 2).

Finally, in the Cretaceous section of the Lusitanian Basin (Portugal), specifically in the early Barremian Papo-Seco Formation (Figuereido et al., 2016), remains of indetermined styracosternan-like ornithopods were described by Figuereido et al. (2022) (Appendix 2).

Based on the current paleobiogeographical knowledge of styracosternan ornithopods from Europe and the Iberian Peninsula and considering the proposed Valanginian-Hauterivian age of the El Horcajo site (Moreno-Azanza et al., 2016), the remains of the styracosternan ornithopod presented here potentially represent the oldest styracosternan remains identified to date in the Iberian Peninsula. The remains of the eastern Cameros sub-basin are about 7.2 million years older than those previously reported from the Iberian Peninsula.

CONCLUSIONS

This paper describes the skeletal remains belonging to ornithopod dinosaurs recovered at the Valanginian-Hauterivian El Horcajo site, in La Rioja, from the Oncala or Enciso groups (Figure 9). These skeletal remains have been assigned to Styracosterna indet. based on the PCA results and on morphological similarities between them and those of other styracosternan ornithopods. This represents the oldest styracosternan remains in the Early Cretaceous of Iberian Peninsula, meaning that styracosternan ornithopods inhabited the area more previously than reported.

ACKNOWLEDGMENTS

This work was supported by La Rioja Government, Spain by “Convenio para la financiacion de actividades de la Catedra Extraordinaria de Patrimonio Paleontologico” in the Universidad de La Rioja, the Basque Government (IT1418-19); Spanish Ministry of Science, Innovation and Universities and the European Regional Development Fund (CGL2017-85038-P); the Universidad del País Vasco/Euskal Herriko Unibertsitatea [PPG17/05]. Erik Isasmendi was supported by a fellowship from the Basque Government/EJ (PRE_2019_1_0215). It is important to highlight the support given by the Dirección General de Cultura (Servicio de Conservación y Promoción del Patrimonio Histórico Artístico), the Reserva de la Biosfera de los valles Leza, Jubera, Cidacos y Alhama and Consejería de Sostenibilidad, Transición Ecológica y Portavocía del Gobierno de La Rioja. We would like to thank Dr. M. Moreno-Azanza for his help during the preparation of this article. We would also would like to thank Dr. F. Torcida Fernández-Baldor (MDS), C.A. Riesgo (MDS), Dr. A. Cobos Periañez (Fundación Conjunto Paleontológico de Teruel-Dinópolis), E.E. Linares (FCPTD), Dr. J.M. Gasulla (Museu Temps de Dinosaures) and to the team of the Museo Numantino (MNS) in allowing us access to several fossils from the museum and giving us permission to use the photographs of these fossils in this work. We would like to thank G. García Martín (UCM) for taking the photographs of the material. We would like to thank Dr. S. Hartman, Dr. D.B. Norman and A. Blázquez Riola for allow-

ing us to use their images and paleoillustrators in this work. Finally, we would like to thank the three anonymous reviewers for their advice and recommendations that have greatly helped in the development and improved the quality of this work.

REFERENCES

Aurell, M., Soria, A.R., Badenas, B., Liesa, C.L., Canudo, J.I., Gasca, J.M., Moreno-Azanza, M., Medrano-Aguado, E., and Meléndez, A. 2018. Barremian synrift sedimentation in the Oliete sub-basin (Iberian Basin, Spain): palaeogeographical evolution and distribution of vertebrate remains. Journal of Iberian Geology, 44, 2:285-308, 285e308. https://doi.org/10.1007/s41513-018-0057-3

Austen, P.A. and Batten, D.J. 2018. English Wealden fossils: an update. Proceedings of the Geologists Association, 129, 2:171-201. https://doi.org/10.1016/j.pgeola.2018.02.007

Baele, J.M., Pascal, G., Spagna, P., and Dupuis, C. 2012. A Short Introduction to the Geology of the Mons Basin and the Iguanodon Sinkhole, Belgium. 3:35-41. In Godefroit P. (ed.), Bernissart dinosaurs and Early Cretaceous terrestrial ecosystems. Indiana University Press, Indiana. https://doi.org/10.2979/6070.0

Barrett, P. 2016. A new specimen of *Valdosaurus canaliculatus* (Ornithopoda: Dryosauridae) from the Lower Cretaceous of the Isle of Wight, England. Memoirs of Museum Victoria, 74:29-48. https://doi.org/10.24199/j.mmv.2016.74.04

Batten, D.J. 2011. Wealden geology. In Batten, D.J. (ed.), English Wealden fossils. London: The Palaeontological Association, 7–14.

Baumel, J.J. and Witmer, L.M. 1993. Osteology. 45-136. In Baumel, J.J., King, A., Lucas Breazile, A., and Evans, H. (eds.), Handbook of avian anatomy: nomina anatomica avium: Cambridge, Massachusetts, Publication of the Nuttall Ornithological Club.

Baur, G. 1891. Remarks on the reptiles generally called Dinosauria. The American Naturalist, 25, 293:434-454.

Berrocal-Casero, M., Barroso-Bercenilla, F., Callapez, P.M., Pimentel, R., Alcalde-Fuentes, M.R., and Prieto, I. 2025. New ornithopod remains from the upper Barremian (Lower Cretaceous) of Vadillos-1 (Cuenca, Spain). Fossil studies 2025, 3, 5. https://doi.org/2813-6284/3/1/5

Bertozzo, F., Dalla-Vecchia F.M., and Fabbri, M. 2017. The Venice specimen of *Ouranosaurus nigeriensis* (Dinosauria, Ornithopoda). PeerJ 5:e3403. https://doi.org/10.7717/peerj.3403

Bonsor, J.A., Lockwood, J.A.F., Leite, J.V., Scott-Murray, A., and Maidment, S.C.R. 2023. The osteology of the holotype of the British Iguanodontian dinosaur *Mantellisaurus atherfieldensis.* Monographs of the Palaeontographical Society, 177:1-63. https://doi.org/10.1080/02693445.2023.2234156

Buffetaut, E. 2004. An *Iguanodon* jaw (Dinosauria, Ornithopoda) from the Lower Cretaceous of Aube (eastern Paris Basin, France), Oryctos, 5:63-68.

Buscalioni, Á.D., Fregenal, M.A., Bravo, A., Poyato-Ariza, F.J., Sanchíz, B., Báez, A.M., Moo, Ó.C., Martín-Closas, C., Evans, S.E., and Marugán-Lobón, J. 2008. The vertebrate assemblage of Buenache de la Sierra (Upper Barremian of Serrania de Cuenca, Spain) with insights into its taphonomy and palaeoecology. Cretaceous Research 29, 4:687-710.

Carpenter, K. and Wilson, Y. 2008. A new species of *Camptosaurus* (Ornithopoda: Dinosauria) from the Morrison Formation (Upper Jurassic) of Dinosaur National Monument, Utah, and a Biomechanical Analysis of its forelimb. Annals of Carnegie Museum 76, 4:227-263.

Chanthasit, P. 2010. The ornithopod dinosaur *Rhabdodon* from the Late Cretaceous of France: anatomy, systematics and paleobiology. Ph.D. dissertation, Université Claude Bernard-Lyon I, Lyon.

Díaz-Martínez, I. 2013. Icnitas de dinosaurios bípedos de La Rioja (Cuenca de Cameros, Cretácico Inferior): icnotaxonomía y aplicación paleobiológica. Unpublished PhD Thesis, Universidad de La Rioja, La Rioja, Spain.

Dieudonné P.E., Tortosa, T., Torcida Fernández-Baldor, F., Canudo J.I., and Díaz-Martínez, I. 2016. An Unexpected Early Rhabdodontid from Europe (Lower Cretaceous of Salas de los Infantes, Burgos Province, Spain) and a Re-Examination of Basal Iguanodontian Relationships. PLoS One 11(6): e0156251. https://doi.org/10.1371/journal.pone.0156251

Dollo, L. 1888. Iguanodontidae et Camptonotidae. Comptes Rendus De Academie Des Sciences, Paris, 106:775-777.

Doublet, S. 2004. Controles tectonique et climatique de l'enregistrement stratigraphique dans un bassin continental de rift: le bassin de Cameros. Unpublished PhD Tesis. Universite de Bourgogne, Dijon, France.

Figueiredo, S., Bachtsevanidou S.I., Rosina, P., and Gomes, M. 2016. New Data about the Paleo Environment of the Papo-Seco Formation (Lower Cretaceous) of Southern Portugal. Journal of Environmental Science and Engineering A, 5:463-470. https://doi.org/10.17265/2162-5298/2016.09.004

Figueiredo, S., Carvalho, I., Pereda-Suberbiola, X., Cunha, P., Bachtsevanidou-Strantzali, I., and Antunes, V. 2022. Ornithopod dinosaur remains from the Papo Seco Formation (lower Barremian, Lusitanian Basin, Portugal): a review of old and new finds. Historical Biology, 35, 11:2181-2192. https://doi.org/10.1080/08912963.2022.2138372

Fuentes-Vidarte, C., Calvo, M., Fuentes, F., and Fuentes, M. 2016. A new styracosternan dinosaur (Ornithopoda: Ankylopollexia) from the Lower Cretaceous of Spain. Spanish Journal of Palaeontology, 31, 2:407-446. https://doi.org/10.7203/SJP.31.2.17163

Forster, C.A. 1990. The Postcranial Skeleton of the Ornithopod Dinosaur *Tenontosaurus tilletti*. Journal of Vertebrate Paleontology, 10, 3:273-294. https://doi.org/10.1080/02724634.1990.10011815

Fregenal-Martínez, M., Meléndez, N., Muñoz-García, M.B., Elez, J., and de la Horra, R. 2017. The stratigraphic record of the Late Jurassic-Early Cretaceous rifting into the Alto Tajo-Serranía de Cuenca region (Iberian Ranges, Spain): Genetic and structural evidences for a revision and a new lithostratigraphic proposal. Revista de la Sociedad Geológica de España 30,1:113-142.

García-Ortiz de Landaluce, E. 2016. Análisis de los yacimientos de icnitas de dinosaurios de La Rioja (N de España) como recurso patrimonial y aplicación de nuevas tecnologías a su estudio. Unpublished PhD Thesis, Universidad de León, León, Spain. https://doi.org/10.18002/10612/5461

García-Cobeña, J., Verdú, F.J., and Cobos, A. 2022. Abundance of large ornithopod dinosaurs in the El Castellar Formation (Hauterivian-Barremian, Lower Cretaceous) of the Peñagolosa sub-basin (Teruel, Spain). Journal of Iberian Geology 2022, 1:107-127. https://doi.org/10.1007/s41513-021-00185-w

García-Cobeña, J., Verdú, F.J., and Cobos, A. 2023. New ornithopod fossils and associated faunas from the upper Hauterivian–lower Barremian (Lower Cretaceous) El Castellar Formation in the Province of Teruel. Journal of Iberian Geology 2024, 50:57-66. https://doi.org/10.1007/s41513-023-00216-8

García-Cobeña, J., Verdú, F.J., and Cobos, A. 2024. Systematic of a Massively Constructed Specimen of *Iguanodon galvensis* (Ornithopoda, Iguanodontidae) from the Early Barremian (Early Cretaceous) of Eastern Spain. Diversity 2024, 9:586. https://doi.org/10.3390/d16090586

Gasca, J., Moreno-Azanza, M., Ruiz-Omeñaca, J., and Canudo, J.I. 2015. New material and phylogenetic position of the basal iguanodont dinosaur *Delapparentia turolensis* from the Barremian (Early Cretaceous) of Spain. Journal of Iberian Geology 2015, 41:57-70. https://doi.org/10.5209/rev_JIGE.2015.v41.n1.48655

Gasulla, J.M., Ortega, F., Sanz, J.L., Escaso, F., and Pérez-García, A. 2010. Un nuevo ejemplar de *Iguanodon bernissartensis* (Dinosauria: Ornithopoda) del Aptiense inferior de Morella (Castellón, España). Publicaciones del Seminario de Paleontología de Zaragoza (SEPAZ), 9:142-145.

Gasulla, J.M., Sanz, J., Ortega, F., Escaso, F., and Pérez-García, A. 2012. Isolated vertebrae of the ornithopod *Mantellisaurus* from the early Aptian of Morella (Spain). EAVP 10th Annual Meeting of the European Association of Vertebrate Palaeontologists, 94.

Gasulla, J.M., Escaso, F., Ortega, F., and Sanz, J.L. 2014. New hadrosauriform cranial remains from the Arcillas de Morella Formation (lower Aptian) of Morella, Spain. Cretaceous Research, 47:19-24. https://doi.org/10.1016/j.cretres.2013.10.004

Gasulla, J.M. 2015. Los dinosaurios de la Cantera del Mas de la Parreta, Morella (Formación Morella, Barremiense superior, Cretácico Inferior): Sistemática, análisis filogenético e implicaciones paleobiológicas. Unpublished PhD Tesis, Universidad Autónoma de Madrid, Madrid, Spain.

Gasulla, J.M., Escaso, F., Narváez, I., Ortega, F., and Sanz, J.L. 2015. A New Sail-Backed Styracosternan (Dinosauria: Ornithopoda) from the Early Cretaceous of Morella, Spain. PLoS ONE 10, 12: e0144167. https://doi.org/10.1371/journal.pone.0144167

Gasulla, J.M., Escaso, F., Narváez, I., Sanz, J.L., and Ortega, F. 2022. New *Iguanodon bernissartensis* Axial Bones (Dinosauria, Ornithopoda) from the Early Cretaceous of Morella, Spain. Diversity 2022, 14, 2:14-63. https://doi.org/10.3390/d14020063

Hammer, Ø., Harper, D.A.T., and Ryan, P.D. 2001. Past: Paleontological Statistics Software Package for Education and Data Analysis. Palaeontologia Electronica, 4.1.4A:1-9. https://palaeo-electronica.org/2001_1/past/past.pdf

Hernán, F.J. 2018. Estratigrafía y sedimentología de las formaciones con icnitas de dinosaurios del Grupo Enciso (Cameros, La Rioja, Aptiense). Unpublished PhD Thesis, Universidad Politécnica de Madrid, Madrid, Spain. https://doi.org/10.20868/UPM.thesis.55957

Hopson, P.M., Wilkinson, I.P., and Woods, M.A. 2008. A stratigraphical framework for the lower cretaceous of England. British Geological survey. British Geological Survey Research Report, 68 pp.

Isasmendi, E., Sáez-Benito, P., Torices, A., Navarro-Lorbés, P., and Pereda-Suberbiola, X. 2020. New insights about theropod palaeobiodiversity in the Iberian Peninsula and Europe: Spinosaurid teeth (Theropoda, Megalosauroidea) from the Lower Cretaceous of La Rioja (Spain). Cretaceous Research 2020,116:104600. http://doi.org/10.1016/j.cretres.2020.104600

Isasmendi, E., Navarro-Lorbés, P., Sáez-Benito, P., Viera, L.I., Torices, A., and Pereda-Suberbiola, X. 2023. New contributions to the skull anatomy of spinosaurid theropods: Baryonychinae maxilla from the Early Cretaceous of Igea (La Rioja, Spain), Historical Biology, 35, 6:909-923. http://doi.org/10.1080/08912963.2022.2069019

Isasmendi, E., Cuesta, E., Díaz-Martínez, I., Company, J., Sáez-Benito, P., Viera, L.I., Torices, A., and Pereda-Suberbiola, X. 2024. Increasing the theropod record of Europe: a new basal spinosaurid from the Enciso Group of the Cameros Basin (La Rioja, Spain). Evolutionary implications and palaeobiodiversity. Zoological Journal of the Linnean Society 2024, 202, 3:1-34. https://doi.org/10.1093/zoolinnean/zlad193

Llandres-Serrano, M., Vullo, R., Morugán-Lobón, J., Ortega, F., and Buscalioni, A. 2013. An articulated hindlimb of a basal iguanodont (Dinosauria, Ornithopoda) from the Early Cretaceous Las Hoyas Lagerstäte (Spain). Geological Magazine, 150, 3:572-576. https://doi.org/10.1017/S0016756813000095

Lockwood, J.A.F., Martill, D.M., and Maidment, S.C.R. 2021. A new hadrosauriform dinosaur from the Wessex Formation, Wealden Group (Early Cretaceous), of the Isle of Wight, southern England. Journal of Systematic Palaeontology, 19, 12:847-888. https://doi.org/10.1080/14772019.2021.1978005

Lockwood, J.A.F., Martill, D.M., and Maidment S.C.R. 2024. *Comptonatus chasei*, a new iguanodontian dinosaur from the Lower Cretaceous Wessex Formation of the Isle of Wight, southern England. Journal of Systematic Palaeontology, 22, 1:1-87. https://doi.org/10.1080/14772019.2024.2346573

Madzia, D., Arbour, V.M., Boyd, C. Farke, A.A., Cruzado-Caballero, P., and Evans, D.C. 2021. The phylogenetic nomenclature of ornithischian dinosaurs. PeerJ, 9:e12362. https://doi.org/10.7717/peerj.12362

Maidment, S.C.R., Chapelle, K.E.J., Bonsor, A., Button, D., and Barret, P.M. 2023. Osteology and relationships of *Cumnoria prestwichii* (Ornithischia: Ornithopoda) from the Late Jurassic of Oxfordshire, UK. Monographs of the Palaeontographical Society, 176, 664:1-55. https://doi.org/10.1080/02693445.2022.2162669

Marsh, O.C. 1881. Classification of the Dinosauria. American Journal of Science, 133, 3:81–86.

Martín-Chivelet, J., López-Gómez, J., Aguado, R., Arias, C., Arribas, J., Arribas, M. A., Aurell, M., Bádenas, B., Benito, M.I., Bover-Arnal, T., Casas-Sainz, A., Castro, J.M., Coruña, F., A de Gea, G., Fornós, J.J., Fregenal-Martínez, M., García-Senz, J., Garófano, D., Gelabert, B., Giménez, J., González-Acebrón, L., Guimerà, J., Liesa, C.L., Mas, R., Meléndez, N., Molina, J.M., Muñoz, J.A., Navarrete, R., Nebot, M., Nieto, L.M., Omodeo-Salé, S., Pedrera, A., Peropadre, C., Quijada, I.E., Quijano, M.L., Reolid, M., Robador, A., Rodríguez-López, J.P., Rodríguez-Perea, A., Rosales, I., Ruiz-Ortiz, P.A., Sàbat, F., Salas, R., Soria, A.R., Suarez-Gonzalez, P., and Vilas, L. 2019. The late Jurassic-early cretaceous rifting. 169-249 pp. In Quesada, C. and Oliveira, J. (eds.), The Geology of Iberia: A Geodynamic Approach. Regional Geology Reviews. Springer.

Martín-Closas, C. 1989. Els caròfits del cretaci inferior de les conques perifèriques del bloc de l'Ebre. Barcelona: Publicacions Universitat de Barcelona, 581 pp.

Martín-Closas, C. and Alonso-Millán, A. 1998. Estratigrafía y bioestratigrafía (Charophyta) del Cretácico inferior en el sector occidental de la Cuenca de Cameros (Cordillera Ibérica). Revista de la Sociedad Geológica de España, 11, 3-4:253-269.

Mas, J.R., Benito, M.I., Arribas, J., Serrano, A., Guimerà, J., Alonso, Á., and Alonso-Azcárate, J. 2002. La Cuenca de Cameros: desde la extensión Finijurásica-Eocretácica a la inversión terciaria-implicaciones en la exploración de hidrocarburos. Zubía, 2002, 14:9-64.

Mas, J.R., Alonso, A., and Guimera, J. 1993. Evolución tectonosedimentaria de una cuenca extensional intraplaca: La cuenca finijurásica-eocretácica de Los Cameros (La Rioja-Soria). Revista de la Sociedad Geológica de España, 6:129-144.

Mas, J.R., Benito, M.I., Arribas, J., Serrano, A., Guimerà, J., Alonso, and Á. y Alonso-Azcárate, J. 2003. The Cameros Basin: From Late Jurassic – Early Cretaceous Extension to Tertiary Contractional Inversión-Implications of Hydrocarbon Exploration, p. 1-52. Geological Field Trip 11. AAPG International Conference and Exhibition. Barcelona (Spain).

McDonald, A.T., Bird, J., Kirkland, J.I., and Dodson, P. 2012a. Osteology of the basal hadrosauroid *Eolambia caroljonesa* (Dinosauria: Ornithopoda) from Cedar Mountain Formation of Utah: PLoS ONE, 7:e45712. https://doi.org/10.1371/journal.pone.0045712

Mcdonald, A., Espilez, E., Mampel, L., Kirkland, J., and Alcalá, L. 2012b. An unusual new basal iguanodont (Dinosauria: Ornithopoda) from the Lower Cretaceous of Teruel, Spain. Zootaxa, 3595:61-76. https://doi.org/10.11646/zootaxa.3595.1.3

Medrano-Aguado, E., Parrilla, J., Gasca, J., Alonso, A., and Canudo, J. 2022. Ornithopod diversity in the Lower Cretaceous of Spain: New styracosternan remains from the Barremian of the Maestrazgo Basin (Teruel province, Spain). Cretaceous Research, 144:105458. https://doi.org/10.1016/j.cretres.2022.105458

Moreno-Azanza, M., Gasca, J.M., Díaz-Martínez, I., Bauluz Lázaro, B., Canudo Sanagustín, J.I., Fernández, A., and Pérez-Lorente, F. 2016. A multi-ootaxic assemblage from the Lower Cretaceous of the Cameros Basin (La Rioja; Northern Spain). Spanish Journal of Palaeontology, 31:305-320. https://doi.org/10.7203/sjp.31.2.17158

Navarro-Lorbés, P. and Torices, A. 2018. Preliminary analysis of theropod teeth from El Horcajo, Lower Cretaceous, La Rioja, Spain, p. 83-86. In Amayuelas, E. (ed.), Life finds a way. Gasteiz.

Norman, D.B. 1980. On the ornithischian dinosaurs *Iguanodon bernissartensis* from the Lower Cretaceous of Bernissart (Belgium). Memoires De L'institut Royal Des Sciences Naturelles De Belgique, 178:1-103.

Norman, D.B. 1986. On the anatomy of *Iguanodon atherfieldensis* (Ornithischia: Ornithopoda). Bulletin-Institut Royal des Sciencies Naturelles de Belgique. Sciences de la Terre, 56:281-372.

Norman, D.B. 1987. A mass accumulation of vertebrates from the Lower Cretaceous of Nehden (Sauerland), West Germany. Proceedings of the Royal Society of London, Series B, Biological Sciences 230, 1259:215-255.

Norman, D.B. 2002. On Asian ornithopods (Dinosauria: Ornithischia). *Probactrosaurus* Rozhdestvensky, 1966. Zoological Journal of the Linnean Society, 136:113-144.
Norman D.B. 2011. On the osteology of the lower Wealden Group (Valanginian) ornithopod *Barilium dawsoni* (Iguanodontia: Styracosterna). Special Papers in Palaeontology, 86:165-194.
Norman, D.B. 2013. On the taxonomy and diversity of Wealden iguanodontian dinosaurs (Ornithischia: Ornithopoda), Revue de Paléobiologie 32, 2:385-404.
Norman, D.B. 2015. On the history, osteology, and systematic position of the Wealden (Hastings group) dinosaur *Hypselospinus fittoni* (Iguanodontia: Styracosterna), Zoological Journal of the Linnean Society, 173, 1:92-189. https://doi.org/10.1111/zoj.12193
Norman, D.B. and Barrett, P.M. 2002. Ornithischian dinosaurs from the lower Cretaceous (Berriasian) of England. Special Papers in Palaeontology, 68:161-189.
Pérez-Lorente, F. 2015. Dinosaur footprints & trackways of La Rioja. Series: Life of the Past. Indiana University Press, Bloomington.
Poole, K.E. 2022. Phylogeny of iguanodontian dinosaurs and the evolution of quadrupedality. Palaeontologia Electronica, 25(3):a30. https://doi.org/10.26879/702
Poyato-Ariza, F.J. and Buscalioni, A.D. 2016. Las Hoyas: A Cretaceous Wetland: A multidisciplinary synthesis after 25 years of research on an exceptional fossil Lagerstätte from Spain. Friedrich Pfeil (ed.), München, 262 pp.
Ramírez-Velasco, A. and Alvarado-Ortega, J. 2022. Guía osteológica de los dinosaurios hadrosauroideos (Ornithopoda, Hadrosauroidea), primera parte: esqueleto postcraneano. Boletín del Instituto de Geología, Universidad Nacional Autónoma de México. Volumen 124, 1:1-51.
Rasmussen, M.E. 1998. The hadrosaurian forelimb morphology, function and inferred phylogeny. Unpublished PhD Thesis. University of Copenhagen. Copenhagen.
Rey, G., Royo-Torres, R., and Alcalá, L. 2018. Nuevos restos de dinosaurios estiracosternos en el Albiense de la Cordillera Ibérica. Geogaceta, 63:83-86.
Riveline, J., Berger, J.P., Feist, M., Martín-Closas, C., Schudack, M., and Soulie-Marsche, I., 1996. European Mesozoic-Cenozoic charophyte biozonation. Bulletin de la Societe geologique de France, 167, 3:453-468.
Rodríguez-López, J.P., Meléndez, N., Soria, A.R., and de Boer, P.L. 2009. Reinterpretación estratigráfica y sedimentológica de las Formaciones Escucha y Utrillas de la Cordillera Ibérica. Revista de la Sociedad Geológica de España, 22:163-219.
Rueden, C.T., Schindelin, J., Hiner, M.C., DeZonia, B.E., Walter, A.E., Arena, E.T., and Eliceiri, K.W. 2017. ImageJ2: ImageJ for the next generation of scientific image data, BMC Bioinformatics, 18:529. https://doi.org/10.1017/s1431927619001442
Ruiz-Omeñaca, J.I. 2001. Dinosaurios hipsilofodóntidos (Ornithischia: Ornithopoda) en la Península Ibérica, p. 175-266. In Colectivo Arqueológico-Paleontológico de Salas (ed.) Actas de las I Jornadas internacionales sobre paleontología de dinosaurios y su entorno. Salas de los Infantes.
Ruiz-Omeñaca, J.I. 2011. *Delapparentia turolensis* nov. gen et sp., un nuevo iguanodontoideo (Ornithischia: Ornithopoda) en el Cretácico Inferior de Galve. Estudios geológicos, 67, 1:83-110. https://doi.org/10.3989/egeol.40276.124
Salas, R., Guimerà, J., Mas, R., Martín-Closas, C., Meléndez, A., and Alonso, A. 2001. Evolution of the Mesozoic Central Iberian Rift System and its Cainozoic inversion (Iberian chain), p 145-185. In Peri-Tethys Memoir 6: Peri-Thetyan Rift/Wrench Basins and Passive Mar gins. Ziegler, P.A., Cavazza, W., Robertson A.H.F., and Crasquin-Soleau (eds.). Memoire du Museum Nationale de Histoire Naturell, 186.
Sanguino, F. and Buscalioni, Á.D. 2018. The *Iguanodon* locality of Pata la Mona (upper Barremian, Buenache de la Sierra, Cuenca) revisited. In Proceedings of the XVI Encuentro de Jóvenes Investigadores en Paleontología, Zarautz, Spain, 11-14 April 2028; pp. 103-106. https://doi.org/10.33414/ajea.1299.2023
Santafé, J.V., Casanovas, M.L., Sanz, J.L., and Calzada, S. 1982. Geología y Paleontología (Dinosaurios) de las Capas rojas de Morella (Castellón, España). Diputación provincial de Castellón y Diputación de Barcelona, p. 169.

Schudack, U. and Schudack, M. 2009. Ostracod biostratigraphy in the Lower Cretaceous of the Iberian chain (eastern Spain) /Bioestratigrafia de ostracodos en el Cretacico Inferior de la Cordillera Iberica (este de Espana). Journal of Iberian Geology, 35, 2:141-168.

Seeley, H.G. 1887. On the classification of the fossil animals commonly named Dinosauria. Proceedings of the Royal Society of London, 43:165-171.

Sereno, P.C. 1986. Phylogeny of the bird-hipped dinosaurs (Order Ornithischia). National Geographic Research, 2:234-256.

Suárez-González, P., Quijada, I.E., Benito, M.I., and Mas, J.R. 2013. Eustatic versus tectonic control in an intraplate rift basin (Leza Fm, Cameros Basin). Chronostratigraphic and paleogeographic implications for the Aptian of Iberia. Journal of Iberian Geology, 39, 2:285-312.
https://doi.org/10.5209/rev_jige.2013.v39.n2.42502

Tischer, G. 1966. Über die Wealden-Ablagerung und die Tektonik der östlichen Sierra de los Cameros in den nordwestlichen Iberischen Ketten (Spanien), p. 123-164. In Beuther, A., Dahm, H., Kneuper-Haack, F., Mensink, H., Tischer, G., Brinkmann, R., De Lôme, D.Y., and Lögters, H. (eds.), Der Jura und Wealden in Nordost-Spanien. Beihefte zum Geologischen Jahrbuch, 44.

Torcida Fernández-Baldor, F. 1996. Registro de dinosaurios en el sureste de la provincia de Burgos. Zubía, 14:89-104.

Torcida Fernández-Baldor, F. 1999. Un dinosaurio iguanodóntido del Cretácico Inferior de Burgos (España). I Jornadas Internacionales sobre Paleontología de dinosaurios y su entorno (resúmenes), Salas de los Infantes, 32.

Torcida Fernández-Baldor, F., Ruiz-Omeñaca, J.I., Izquierdo, L.A., Huerta, P., Montero, D., and Pérez, G. 2003. Nuevos restos de dinosaurios hipsilophodóntidos (ornitischia: ornithopoda) en el Cretácico Inferior de Burgos (España). Geotemas (Madrid), 6, 5:43-46.

Torcida Fernández-Baldor, F., Izquierdo, L.A., Contreras, R., Huerta, P., Montero, D., Pérez, G., and Urién, V. 2006. Un dinosaurio “iguanodóntido” del Cretácico Inferior de Burgos (España), p. 349-363. In Colectivo Arqueológico-Paleontológico Salense, (ed.) Actas de las III Jornadas sobre Dinosaurios y su Entorno. Salas de los Infantes, Burgos, España.

Verdú, F.J. 2017. Sistemática, filogenia y paleobiología de *Iguanodon galvensis* (Ornithopoda, Dinosauria) del Barremiense inferior (Cretácico Inferior) de Teruel (España). Unpublished PhD Thesis, Universitat de València, València, Spain.

Verdú, F.J., Cobos, A., Royo-Torres, R., and Alcalá, L. 2019. Diversity of large ornithopod dinosaurs in the upper Hauterivian-lower Barremian (Lower Cretaceous) of Teruel (Spain): a morphometric approach. Spanish Journal of Palaeontology, 34:269-288.
https://doi.org/10.7203/sjp.34.2.16116

Verdú, F.J., Royo-Torres, R., Cobos, A., and Alcalá, L. 2015. Perinates of a new species of *Iguanodon* (Ornithischia: Ornithopoda) from the lower Barremian of Galve (Teruel, Spain). Cretaceous Research, 56:250-264.
https://doi.org/10.1016/j.cretres.2015.05.010

Yans J., Dejax J., Pons, D., Taverne, L., and Bultynck, P. 2006. The iguanodons of Bernissart (Belgium) are middle Barremian to earliest Aptian in age, Bulletin de l'Institut Royal des Sciences Naturelles de Belgique, Science de la Terre, 76:91-95.

Weishampel, D.B., Jianu, C.M., Cziki, Z., and Norman, D.B. 2003. Osteology and phylogeny of *Zalmoxes* (n. g.), an unusual ornithopod dinosaur from the latest Cretaceous of Romania. Journal of Systematic Paleontology, 1:123-143.

APPENDIX 1.

Table of distributions of styracosternan ornithopods in the sedimentary basins and geological formations of the Early Cretaceous of Europe (excluding the Iberian Peninsula).

Sedimentary basin + Sub-basin + Geological formations / Chronostratigraphic age + Geochronologic age		Vectian Basin		Mons Basin	Paris Basin		Rhenish Massif
		Weald sub-basin	Wessex sub-basin				
		Wadhurst Clay Fm + Weald Clay Fm + Tunbridge Wells Sand Fm	Vectis Fm + Wessex Fm (upper part outcrops in Isle of Wight)	Sainte-Barbe Clays Fm	Calcaire à Spatangues Fm	Argiles Ostreénes Fm	"Nehden Clays"
Albian	Late						
	Early						
Aptian	Late						■ X
	Early		X ■ ■				
Barremian	Late			■		■	
	Early						
Hauterivian	Late				■		
	Early						
Valanginian	Late	●					
	Early	● ●					
Berriasian	Late						
	Early						

■ *Iguanodon bernissartensis* (Norman, 2011, 2015)
■ *Iguanodon bernissartensis* (Norman, 1980; Yans *et al.*, 2006)
■ *Iguanodon bernissartensis* (Norman, 1987)
■ *Iguanodon* sp. (Buffetaut, 2004)
■ *Brighstoneus simmondsi* (Lockwood *et al.*, 2021)

● *Barilium dawsoni* (Norman, 2011)
● *Hypselospinus* cf. *fittoni* (Norman, 2015)
● *Hypselospinus fittoni* (Norman and Barret, 2002; Norman, 2013, 2015)
X *Mantellisaurus atherfieldensis* (Norman, 1987)
X *Mantellisaurus atherfieldensis* (Norman, 1986; Bonsor *et al.*, 2023)

APPENDIX 2.

Table of distributions of styracosternan ornithopods in the sedimentary basins and geological formations of the Early Cretaceous of the Iberian Peninsula. (*): The age marked in discontinuous line for the Oncala or Enciso groups refers to the dating by Moreno-Azanza et al. (2016) (Valanginian-Hauterivian).

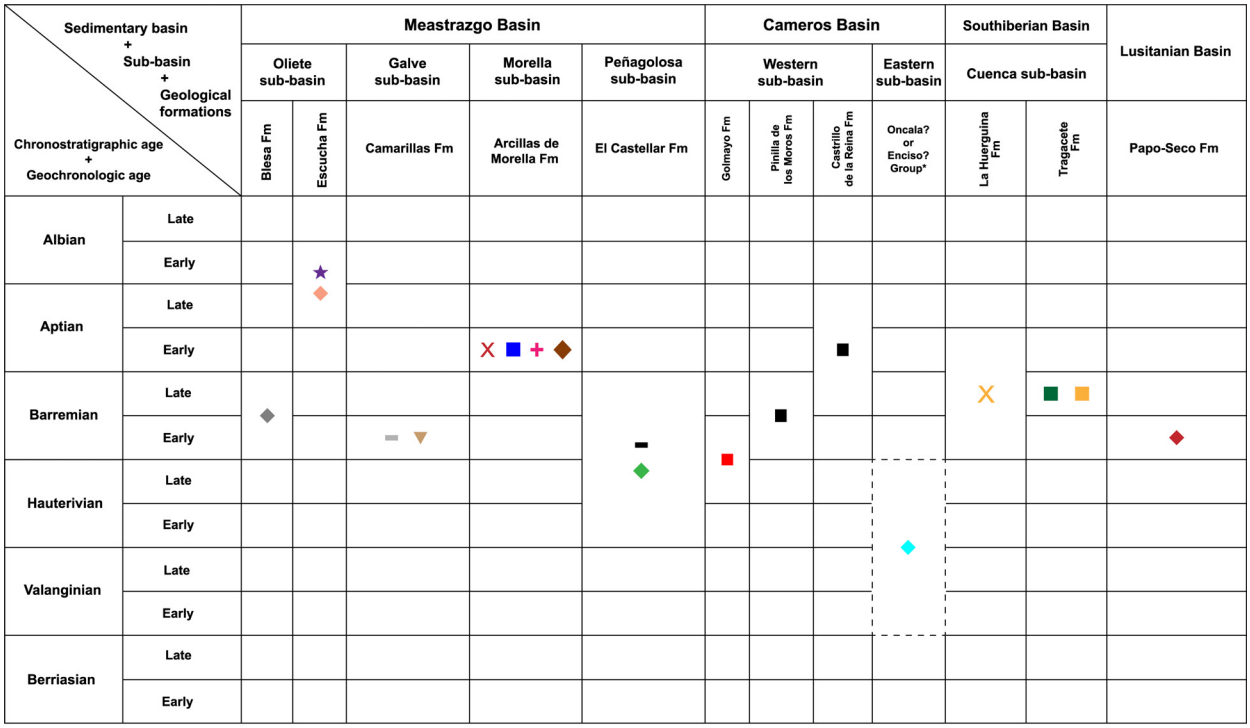

- *Iguanodon bernissartensis* (Gasulla *et al.*, 2010, 2014, 2022; Gasulla, 2015)
- *Iguanodon bernissartensis* (Sanguino and Buscalioni, 2018)
- *Iguanodon* cf. *bernissartensis* (Berrocal-Casero et al., 2025)
- Iguanodontidae indet. (Torcida Fernández-Baldor *et al.*, 1996, 1999, 2006)
- *Magnamanus soriaensis* (Fuentes-Vidarte *et al.*, 2016)
- *Iguanodon galvensis* (Verdú *et al.*, 2015, 2017, 2018; García-Cobeña *et al.*, 2024)
- *Iguanodon* cf. *galvensis* (García-Cobeña *et al.*, 2022)
- *Delapparentia turolensis* (Ruiz-Omeñaca, 2011; Gasca *et al.*, 2015)
- *Morelladon beltrani* (Gasulla *et al.*, 2015)
- *Mantellisaurus atherfieldensis* (Gasulla *et al.*, 2012; Gasulla, 2015)
- *Mantellisaurus atherfieldensis* (Llandres-Serrano *et al.*, 2013)
- *Proa Valdearinnoensis* (McDonald *et al.*, 2012)
- Styracosterna indet. (Gasulla, 2015)
- Styracosterna indet. (Rey *et al.*, 2018)
- Styracosterna indet. (Verdú *et al.*, 2019; García-Cobeña *et al.*, 2022, 2023)
- Styracosterna indet. (Medrano-Aguado *et al.*, 2022)
- Styracosterna indet. (Figuereido *et al.*, 2022)
- Styracosterna indet. (This work)

APPENDIX 3.

Table of specimens examined first-hand. Contains the taxa of ornithopod dinosaurs, the acronyms of the fossils referred to these taxa and their respective references. Spreadsheet available for download at https://palaeo-electronica.org/content/2025/5599-styracosternan-of-la-rioja

APPENDIX 4.

Principal Component Analysis Data Matrix. Contains tables with the measurements of the caudal vertebrae of the ornithopod taxa examined, as well as the results of the PCA. Spreadsheet available for download at https://palaeo-electronica.org/content/2025/5599-styracosternan-of-la-rioja